HHS Public Access

Author manuscript

Brain Behav Immun. Author manuscript; available in PMC 2021 March 23.

Published in final edited form as:

Brain Behav Immun. 2021 January ; 91: 350–368. doi:10.1016/j.bbi.2020.10.013.

Microbiota metabolites modulate the T helper 17 to regulatory T cell (Th17/Treg) imbalance promoting resilience to stress-induced anxiety- and depressive-like behaviors

Susan Westfall[a], **Francesca Caracci**[a], **Danyue Zhao**[c,1], **Qing-li Wu**[c], **Tal Frolinger**[a], **James Simon**[c], **Giulio Maria Pasinetti**[a,b,*]

[a]Icahn School of Medicine at Mount Sinai, Department of Neurology, New York, NY, USA

[b]Geriatric Research, Education and Clinical Center, James J. Peters Veterans Affairs Medical Center, Bronx, NY, USA

[c]Department of Plant Biology, Rutgers University, New Brunswick, NJ, USA

Abstract

Chronic stress disrupts immune homeostasis while gut microbiota-derived metabolites attenuate inflammation, thus promoting resilience to stress-induced immune and behavioral abnormalities. There are both peripheral and brain region-specific maladaptations of the immune response to chronic stress that produce interrelated mechanistic considerations required for the design of novel therapeutic strategies for prevention of stress-induced psychological impairment. This study shows that a combination of probiotics and polyphenol-rich prebiotics, a synbiotic, attenuates the chronic-stress induced inflammatory responses in the ileum and the prefrontal cortex promoting resilience to the consequent depressive- and anxiety-like behaviors in male mice. Pharmacokinetic studies revealed that this effect may be attributed to specific synbiotic-produced metabolites including 4-hydroxyphenylpropionic, 4-hydroxyphenylacetic acid and caffeic acid. Using a model of chronic unpredictable stress, behavioral abnormalities were associated to strong immune cell activation and recruitment in the ileum while inflammasome pathways were implicated in the prefrontal cortex and hippocampus. Chronic stress also upregulated the ratio of activated proinflammatory T helper 17 (Th17) to regulatory T cells (Treg) in the liver and ileum and it was predicted with ingenuity pathway analysis that the aryl hydrocarbon receptor (AHR) could be driving the synbiotic's effect on the ileum's inflammatory response to stress. Synbiotic treatment

*Corresponding author at: Icahn School of Medicine, Annenberg Building, 20-06, 1468 Madison Avenue, New York, NY 10029, USA. giulio.pasinetti@mssm.edu (G.M. Pasinetti).

[1]Current Address: Department of Applied Biology and Chemical Technology, The Hong Kong Polytechnic University, Hong Kong.

Authors Contributions

S.W. planned, designed and implemented all of the experimental procedures and wrote the manuscript. F.C. assisted in all aspects of experimental design and implementation. T.F. developed and assisted in conducting the CUS protocol. D.Z., Q.W. and J.S. conducted the metabolite quantification for the bioavailability and pharmacokinetics. G.M.P. acquired funding and oversaw all aspects of study design, implementation and manuscript preparation.

Declaration of Competing Interest

The authors declare that they have no known competing financial interests or personal relationships that could have appeared to influence the work reported in this paper.

Appendix A. Supplementary data

Supplementary data to this article can be found online at https://doi.org/10.1016/j.bbi.2020.10.013.

indiscriminately attenuated the stress-induced immune and behavioral aberrations in both the ileum and the brain while in a gut-immune co-culture model, the synbiotic-specific metabolites promoted anti-inflammatory activity through the AHR. Overall, this study characterizes a novel synbiotic treatment for chronic-stress induced behavioral impairments while defining a putative mechanism of gut-microbiota host interaction for modulating the peripheral and brain immune systems.

Keywords

Gut-brain-axis; Gut microbiota; Adaptive immunity; Regulatory T cells; Th17 cells; Neuroinflammation; Polyphenols; Metabolome; Psychiatric disorders; Aryl hydrocarbon receptor

1. Introduction

Chronic stress and its corresponding physiological adaptations are major drivers of stochastic depression and anxiety. During times of acute stress, the body initiates physiological processes including hypothalamic–pituitaryadrenal (HPA) axis activation, glucocorticoid release, modulated catecholamine signaling and temporary cytokine and chemokine induction to bring the body back into homeostasis. Under conditions of chronic stress, chronic allostasis becomes allostatic overload, a general “wear and tear” that does not appropriately attenuate the adaptive response to stress when it is no longer required (McEwen, 2004). Major consequences of allostatic overload are neuronal atrophy in regions controlling memory and executive function, including the prefrontal cortex and hippocampus, and the simultaneous hypertrophy in the amygdala leading to elevated anxiety and aggression (McEwen, 2004). Allostatic overload is measured as a multisystem dysfunction in HPA axis, immune, anabolic and cardiovascular functions and has been associated with anxiety and depression in aging adults (Kobrosly et al., 2014; Ullmann et al., 2019). This multisystem consideration has hindered the mechanistic understanding consequently effective therapeutic development for chronic-stress induced behavioral impairments. In the current study, a progressive approach was taken to show how a gut microbiota-modifying synbiotic can simultaneously modulate the peripheral and brain abnormalities characteristic of chronic stress induced immune and behavioral impairments supporting a potential new therapeutic paradigm for psychological stress.

The gut microbiota has become an emerging player in the body’s physiological response to stress (Wiley et al., 2017) with neurological consequences (Westfall and Pasinetti, 2019). Seminal studies showed that fecal transplants from naïve NIH Swiss mice into germ-free BALB/c mice conferred anxiety behaviors (Bercik et al., 2011), while fecal transplant from MDD patients into germ-free mice induced depressive-like behaviors in the recipient mice (Zheng et al., 2016). Recent studies have validated this effect where fecal transplant from chronically stressed into antibiotic-treated mice transferred the neuroinflammatory and psychological impairment characteristic of the donor mice (Li et al., 2019), while the psychological characteristics typical of psychosocial stress have been correlated to the transfer of specific gut microbiota species, especially *Heliobacter* spp. (Langgartner et al., 2017). Correspondingly, the gut microbiota is often disrupted in psychiatric populations

(Jiang et al., 2015; Naseribafrouei et al., 2014), although few studies have identified specific microbiota populations associated with psychiatric symptoms (Valles-Colomer et al., 2019). Recent murine studies have revealed that chronic restraint stress can impose unique dysbiotic characteristics in the mucosa- and lumina-associated microbiomes (Galley et al., 2014). A *meta*-analysis of ten interventional probiotic studies revealed that despite probiotics not impacting depression symptoms in healthy individuals, probiotics improved moods of individuals with mild to moderate depressive symptoms (Ng et al., 2018). Another recently emerging trend is the use of synbiotics for the management of psychiatric disorders. Synbiotics are a combination of probiotics and prebiotics that facilitate production of bioactive metabolites with therapeutic potential (Westfall and Pasinetti, 2019). One clinical study showed that a synbiotic elicited psychological benefits in the Hospital Anxiety and Depression Scale (HADS) to a group of patients with depressive-like symptoms. In addition, the synbiotic slightly elevated serum brain derived neurotrophic factor (BDNF) levels, a biomarker of anxiety, depression and poor synaptic plasticity (Haghighat et al., 2019) validating the psychological and neurochemical benefits of a synbiotic.

The gut microbiota produces a host of bioactive metabolites that can alter the body's homeostatic state allowing it to react to stressful conditions in a more adaptive manner (Westfall and Pasinetti, 2019). Generally classified as gut-brain-axis mechanisms, some of these adaptations include immunomodulatory responses, an increase in antioxidant potential, increased integrity of both gut epithelial and blood–brain-barriers (BBB), sustained parasympathetic tone through vagal signaling and as recently demonstrated, maintenance of synaptic plasticity and cognitive function (Maqsood and Stone, 2016). The gut microbiota also influences neurotransmitters' abundances (Desbonnet et al., 2015; Mayer et al., 2015) that can either cross the BBB or act locally on enterochromaffin cells transducing chemosensory information to the nervous system (Bellono et al., 2017). Tryptophan metabolism into either kynurenine or serotonin is a particularly important pathway for the onset of depression, which is controlled by the gut microbiota (Dehhaghi et al., 2019). In a proinflammatory environment, like a state of chronic stress, there is a shift to higher kynurenine production and consequently, its downstream metabolites that have neurotoxic effects, including quinolinic acid (QA) (Gao et al., 2018). Kynurenine is also a potent agonist of the aryl hydrocarbon receptor (AHR): a transcription factor with an array of xenobiotic functions that also modulates intestinal immunity (Gao et al., 2018) with implications in anxiety- (Kim and Jeon, 2018) and depressive-like behavior in mice (Zang et al., 2018).

The immune system also links the gut microbiota to the development of neuropsychiatric conditions including depressive- and anxiety-like behaviors (Thaiss et al., 2016). Intestinal epithelial cells orchestrate the host's reaction to potential immunological threats as the gut microbiota and its associated metabolites control the integrity and reactivity of these cells. An important part of this response is the programming of naïve lymphocytes and monocytes into their effector subtypes (Britanova and Diefenbach, 2017; Blander et al., 2017). Dendritic cells and monocytes, which form the first tier of the innate immune response, are embedded in the gastrointestinal (GI) associated lymphoid tissue (GALT) and respond directly to the gut microbiota and its metabolites. Based on this interaction, the dendritic cells and monocytes secrete either anti- or pro-inflammatory cytokines and chemokines

creating a distinct inflammatory milieu supporting differentiation of progenitor lymphocytes residing in the mesenteric lymph nodes and Peyer's patches (Koboziev et al., 2010). Of particular interest, specific gut microbiota metabolites alter proinflammatory T helper 17 (Th17) to anti-inflammatory regulatory T cell (Treg) ratios (Arpaia et al., 2013; Luo et al., 2017; Cui et al., 2018; Britton et al., 2019) and the imbalance of Th17 to Treg cells has been implicated in the development of chronic stress-induced depression in mice (Hong et al., 2013). This suggests that gut microbiota-specific metabolites may promote resilience to stress-induced neuropsychiatric disorders by invoking adaptive changes to the immune response through specific lymphocyte subtype expansion. One potential mechanism driving this microbial-derived metabolite to immune regulation could be the AHR. *Ex vivo*, an AHR agonist modulated the activity of human dendritic cells that ultimately supported the differentiation of naïve $CD4^+$ T cells into Tregs (Jurado-Manzano et al., 2017), while knockdown of AHR in a murine splenic $CD4^+$ naïve cell model prevented the modulation of the Treg to Th17 ratio (Shi et al., 2020). *In vivo*, an isoquinoline alkaloid demonstrated anti-arthritic effects by acting as an AHR agonist in intestinal tissues (Tong et al., 2016), while the gut microbiota derived tryptophan metabolite indole-3-aldehyde balanced mucosal reactivity and protected its integrity through AHR-dependent IL-22 secretion (Zelante et al., 2013). While AHR activation tends to promote a protective, Treg-dominating effects, it is important to note that AHR activation is promiscuous and under the right microenvironment can promote a proinflammatory environment and Th17 differentiation (Veldhoen et al., 2008; Quintana et al., 2008). With this evidence, the AHR is acts as a potential crosstalk mediator between gut microbiota derived metabolites and the adaptive immune system in the gut; however, this has not been validated *in vivo* or in a model of stress-induced psychological impairment.

The present study shows that synbiotic-derived metabolites can be developed as an efficacious therapy for stress-induced depressive- and anxiety-like behavior. The synbiotic is composed of a grape-derived prebiotic known as the Bioactive Dietary Polyphenol Preparation (BDPP) and a combination of the probiotics *Lactobacillus plantarum* and *Bifidobacterium longum.* BDPP has been previously shown by our group to produce a battery of microbial-derived bioactive metabolites (Frolinger et al., 2019) that cross the BBB and promote psychological resilience (Frolinger et al., 2018; Wang et al., 2018). The selected *L. plantarum* strain has been extensively characterized as an anti-inflammatory probiotic that interacts with dietary prebiotics (van den Nieuwboer et al., 2016) while *B. longum* strains has been shown to have anti-depressant gut-brain-axis modulating activities (Pinto-Sanchez et al., 2017). Using this combination as a synbiotic, we showed that the synbiotic-derived metabolites were more potent than the BDPP or probiotics alone at reducing the multiplexity of stress-induced neuropathologies and their associated neuroinflammatory phenotypes and dysregulation. This manuscript also presents evidence suggesting that the battery of synbiotic-derived polyphenolic metabolites may signal through the AHR impacting the Th17/Treg cell ratio, altering the peripheral immune profile driving the neuroinflammation characteristic of stress-induced anxiety- and depressive-like behaviors.

2. Materials and methods

2.1. Bacterial cell lines

The bacterial cell lines *Lactobacillus plantarum* ATCC 793 (NCIMB 8826, Hayward 3A, WCFS1) and *Bifidobacterium longum* ATCC 15707 (E194b, Variant a) were cultivated from frozen stock in Man-Rogosa-Sharpe (MRS) media and MRS with 0.05% cysteine, respectively, in an anaerobic incubator at 37 °C. Bacterial stocks were maintained at −80 °C in a 20% glycerol stock. Routine cultures were maintained by 1% *v*/*v* inoculate, grown for 18 h and renewed from the frozen stock weekly to ensure culture purity.

2.2. Animal husbandry & treatment

C57BL/6J male mice were purchased from The Jackson Laboratory (age 8 wk; Bar Harbor, ME, USA) and group housed (4 mice/cage) in the centralized animal care facility of the Center for Comparative Medicine and Surgery at the Icahn School of Medicine at Mount Sinai. All animals were maintained on a 12-h light/dark cycle with lights on at 07:00 am in a temperature-controlled (20 ± 2 °C) vivarium with access to food and water *ad libitum.* All procedures, protocols and behavioral experiments were approved by the Mount Sinai Institutional Animal Care and Use Committee (IACUC). Female mice were excluded from the study as chronic stress-induced behavioral deficits are sex dependent and require different behavioral paradigms to invoke comparable stress-induced behavioral and immunological phenotypes (Hodes et al., 2015). The current study can only conclude results in male mice and future studies will be conducted to directly compare sex differences.

During pretreatment and for the duration of the protocols, animals were fed a polyphenol-free diet whose composition is outlined in Table S1. Following the 2-week stabilization and acclimatization period for the mice, all animals were placed on their respective treatment (control, BDPP only, probiotic only or synbiotic) for 2 weeks prior to starting the stress protocol. The Bioactive Dietary Polyphenol Preparation (BDPP) was comprised of 1% *w*/*v* grape seed polyphenol extract (GSPE; Healthy Origins), 1% *w*/*v* resveratrol (BulkSupplements.com) and a 5% *w*/*v* concord grape extract (AA Pharmachem, San Diego, USA) made in sterile water. All tested compounds were analyzed by liquid chromatography–mass spectrometry and archived as previously reported (Frolinger et al., 2018) in compliance with National Institutes of Health, National Center for Complementary and Integrative Health (Bethesda, MD, USA) product integrity guidelines.

Probiotic doses for mice were prepared by growing cultures in bulk as previously described, centrifugation at 4000 rpm, 4 °C for 10 min, washing the bacterial pellet with sterile PBS and reconstituting the washed pellet to a 100 X concentrated dose, based on a previously calculated standard curve (colony forming unit (CFU) vs. OD600nm). The bacteria were incorporated into the animals' water at a final dosage of 1.0×10^9 CFU/day per bacterium, calculated based on the average daily water consumption per cage, which was recalculated and replaced daily. Probiotic viability in water and BDPP solution was validated to be 80% +/− 3% after 24 h, with no significant difference in viability between probiotics in water or BDPP solutions. Probiotic's were not gavaged as this daily stressor was deemed a confound

in this experiment which was evaluating stress. The synbiotic was composed of a combination of BDPP and the probiotic combination and was also replaced daily.

2.3. Chronic unpredictable stress (CUS) protocol

To assess the effect of synbiotic treatment on depressive- and anxiety-like behaviours in a model of chronic unpredictable stress (CUS), mice were randomly subdivided into 8 treatment groups ($n = 12–16$) including untreated control (Control), BDPP-only (BDPP), probiotic or synbiotic either stressed or not-stressed. Control groups contained $n = 12$ animals where stressed groups contained $n = 16$ animals and all animals were included in the final analysis. Treatment with the respective supplementation (BDPP, probiotics or synbiotics) were initiated 2 weeks prior to the initiation of the stress protocol. Animals were then subjected to CUS for 28 days that consisted of a random combination of two stressors per day separated by at least 4 h, when possible, yet always when an acute stress was presented (Table S2). Stressors included 45° cage tilt for 12 h, wet bedding for 10–12 h, no bedding for 10–12 h, food and/or water deprivation for 12 h, 4 °C cold exposure for 1 h, cold water swim for 5 min, cage shaking for 20 min, reversed light schedule, restraint stress for 1 h or crowding with 12 animals/cage for 1 h. Animals' food consumption and weight were monitored weekly while water consumption for the BDPP, probiotic and synbiotic groups were recorded daily. No significant changes between groups were observed for the weight, water or food consumption throughout the testing period and the animals gained weight as expected throughout the testing paradigm (Fig. S1). At day 26, animals were subjected to the open field assessment for anxiety-like behavior while day 28, animals were subjected to the forced swim test for depressive-like behavior. Animals were sacrificed immediately following the forced swim test, blood was collected by cardiac puncture into heparinized tubes while dissected tissues were immediately stored on dry ice and stored at −80 °C until analysis.

2.4. Behavioral experiments

Behavioral experiments were performed with a NIR camera and measured with ANY-maze™ tracking software (Stoelting Co., IL, USA. Version 5.1 Beta). All animals were handled for 5 min/day for 3 days prior to behavioral testing to acclimatize them to the experimenter's hands. Before each assessment, mice were habituated to the testing room for 1 h at the beginning of the test day. All tests were conducted by the same experimenter at 8–9:30 AM and conducted in 3 batches. Behavioral assessments were also controlled for potential cage-specific trends including the confound of coprophagia; however no significant differences between the depressive- or anxiety-like behaviors was observed between cages of the same group of mice or conducted on different days.

The open field test for anxiety-like behavior was conducted in four chambers simultaneously, and each chamber measured 40 cm (length) × 40 cm (width) and 38 cm (height) made from high density non-porous plastic completely covered in white paper to remove contextual cues. Each chamber was equally illuminated with a supplementary bright white light. A single downward facing camera tracked the four chambers simultaneously. The recording was started immediately after the mice were placed in center of the apparatus and mice were allowed to explore the chambers during a ten min test. The first minute was

excluded from the analysis for all tests (Seibenhener and Wooten, 2015). The center measure was recorded as a centered 10 cm × 10 cm square and the time that the animal's head spent in the center compartment was assessed as a measure of anxiety (Seibenhener and Wooten, 2015). Total distance travelled was used a control of mobility and no significant variations were observed between treatment groups.

The forced swim test for depressive-like behavior was conducted simultaneously with four apparatuses with two side-facing cameras under ambient light conditions. Mice were tested in 4 L Pyrex glass beakers with a 16 cm diameter, containing 2 L of water stabilized to room temperature (20 + 1 °C) overnight. Animals' behavior was monitored for 6 min with the first minute being excluded from the analysis (Can et al., 2012). The amount of time that the animals were completely immobilized was considered a measure of depressive-like behavior. This study did not use the sucrose preference test as a measure of depressive-like behavior as the BDPP solution, although mostly devoid of sugar, does offer a different taste sensation compared to water or probiotics alone, introducing a confound to the results of the sucrose preference test.

2.5. Bioavailability and pharmacokinetics

Bioavailability of the chronically-dosed BDPP- and synbiotic-derived metabolites was conducted by subjecting 6 week-old male mice ($n = 6$) to the polyphenol-free diet for 2 weeks followed by 3 weeks of either BDPP- or synbiotic- treatment as previously described. Prior to the chronic time-points, mice were housed without food or water for 12 h prior to a bolus dose of the equivalent of one daily dose of BDPP or synbiotic administered through oral gavage. Animals were sacrificed 0.25, 0.5, 1, 2, 4, 8 and 24 h following the bolus dose where after 4 h, animals were given regular food and water. Animals were sacrificed either by asphyxiation followed by cardiac puncture for the collection of blood or by a ketamine (100 mg/kg) - xylazine (12.5 mg/kg) mix followed by cardiac perfusion with saline for the collection of brain samples. Blood was collected in heparinized tubes and stored in a formic acid with a final concentration of 2%. Similarly, brain samples after collected were immediately homogenized in a 2% formic acid solution and frozen at −80 °C until analysis.

2.6. Extraction and chemical profiling of BDPP-derived polyphenols and their metabolites

The analysis of BDPP-derived phenolic compounds was conducted as per previously reported (Ho et al., 2019) with modifications. Briefly, acidified and homogenized plasma and brain samples were thawed on ice and then processed at room temperature. Two internal standards (ISs), *trans*-cinnamic acid-d_7 and 4-hydroxybenzoic-2, 3, 5, 6-d_4, were mixed (each at 2 μg/mL) were diluted in 0.4 M NaH_2PO_4 buffer (pH 5.0) and added to an aliquot (200 μL for plasma and 500 μL for brain). The samples were then incubated with 100 μL (plasma) or 200 μL (brain) of β-glucuronidase solution (2000 U, in contamination with sulfatase) at 37 °C for 45 min after purging with nitrogen. Enzymatic reaction was stopped by adding ethyl acetate (500 μL). Each sample mixture was then sonicated in an ice water bath for 5 min, followed by centrifugation at 8,000 xg for 5 min. The upper organic phase was transferred to a glass test tube. After two more extractions with ethyl acetate, the pooled supernatant was mixed with 20 μL of 2% ascorbic acid and dried using a Savant Speed Vac Concentrator (Farmingdale, NY, USA). The residue was reconstituted in 100 μL of 60%

methanol containing 0.1% formic acid and centrifuged at 16,500 xg for 10 min prior to LC-MS analysis.

Chemical profiling of BDPP-derived polyphenols and their metabolites were carried out using an Agilent 1290 Infinity II UPLC system interfaced with an Agilent 6470 triple quadrupole mass spectrometer with an electrospray ionization (ESI) source (Agilent Technology, Palo Alto, CA, USA). Chromatographic separation was achieved using a Waters Acquity UPLC BEH C18 column (2.1 × 50 mm, 1.7 μm) (Milford, Massachusetts, USA) equipped with a Waters VanGuard Acquity C18 guard column (2.1 × 5 mm, 1.7 μm). The binary mobile phase system consisted of phase A (0.1% AA in water) and phase B (0.1% AA in ACN). Mass spectral data acquisition was achieved under dynamic multiple reaction monitoring (dMRM) mode with switching polarities. For each sample extract, 5 μL was injected into the system in duplicate. Identification and confirmation of target compounds were determined by comparing their MRM precursor-product ion pair transition(s) and the retention time with those of authentic standards. Detailed compound information and MRM transitions are displayed in Table S3. Quantitation was achieved with calibration curves established using the peak area ratio of analyte-to-IS of the quantifier ions.

2.7. RNA extraction and real time PCR

RNA was extracted using the RNeasy kit (Qiagen) and cDNA synthesis was conducted with the High-Capacity cDNA Reverse Transcription Kit with RNase Inhibitor (ThermoFisher) from 1 ug of RNA. qPCR was conducted in collaboration with the Quantitative PCR CoRE at the Icahn School of Medicine at Mount Sinai using an ABI 7900HT Real-Time instrument and SDS software. Relative gene expression was assessed using the delta-delta CT method (Livak and Schmittgen, 2001) and all primer pairs and annealing temperatures are provided in Table S4.

2.8. Protein extraction and ELISA assays

Protein from the prefrontal cortex, cortex, hippocampus, liver and ileum were homogenized in RIPA buffer (Sigma) with an added protease inhibitor cocktail (Sigma) and phenylmethylsulfonyl fluoride (PMSF) phosphatase inhibitors (ThermoFisher) and allowed to extract at 4 °C for 30 min. The concentration of centrifuged supernatants were quantified using the BCA protein assay kit (Pierce, ThermoFisher) and aliquots of 10 mg/ml proteins were made prior to storage at −80 °C. ELISA assays for the cytokines IL-1β, IL-10 (R&D Biosystems), IL-6 (ThermoFisher) and IL-17A (ThermoFisher) were conducted from samples thawed on ice.

2.9. Nanostring multiplex assay

The NanoString multiplex gene expression analysis was conducted in collaboration with the Quantitative PCR CoRE at the Icahn School of Medicine at Mount Sinai and analyzed with the nSolver version 4.0 software. All groups were assessed using the nCouter Mouse Neuroinflammatory Panel in triplicate. Further downstream network and pathway analysis was conducted with the use of Ingenuity Pathway Analysis (IPA; QIAGEN Inc.). The Nanostring data set was deposited in NIH's GEO database GSE148579.

2.10. Single cell suspension and flow cytometry

Single cell suspensions of the liver, spleen and PBMCs were made for the flow cytometry experiments. Animals were sacrificed by carbon dioxide asphyxiation. Blood was drawn by cardiac puncture and immediately placed in EDTA-coated blood collection tubes on ice. PBMCs were extracted by mixing whole blood with RBC lysis buffer for 10 min on ice. Samples were then made up to 10 mL with HBSS (without Ca/Mg), centrifuged at 1200 rpm for 5 min at 4 °C and the process repeated for the pellets until all red blood cells were removed. The liver and ileum (distal 5 cm of the small intestine) were removed and placed in RPMI supplemented with FBS (2%) and HEPES (1X) on ice. The liver was washed, cut into small pieces and placed in a digestion buffer containing RPMI supplemented with FBS (5%), DNase I (0.5 mg/mL) and collagenase IV (0.4 mg/mL) and immediately placed at 37 °C for 30 min with agitation. After 30 min, the liver was pulverized with a 18G needle and filtered through a 100 μM mesh on ice. Ileum samples were washed in PBS to remove fecal matter and cut longitudinally so mucus and remaining fecal matter could be removed. The whole ileum was placed in a dissociation buffer of RPMI supplemented with FBS (5%), EDTA (5 mM) and HEPES (1X) for 30 min at 37 °C with agitation. Following the 30 min, the ileum was transferred to a digestion buffer of RPMI supplemented with FBS (5%), DNase I (0.5 mg/mL) and collagenase VIII (0.4 mg/mL) and incubated a further 25 min at 37 °C with agitation. Like the liver, the ileum was pulverized with a 18 G needle and filtered through a 100 μM mesh onto ice. Both the liver and ileum were centrifuged at 1200 rpm for 5 min at 4 °C, RBCs were lysed and the samples washed a further two times in HBSS to remove debris. Samples were resuspended in PBS and stained with the live/dead yellow fixable dye (1 μL / 1 mL resuspended cells). Samples were incubated for 30 min on ice and washed once in staining buffer (PBS and 5% bovine serum albumin). Surface markers CD3ε (clone 145–2C11, PE-CY7, Biolegend, RRID:AB_312685), CD4 (clone RM4–5, APC Cy7, Biolegend, RRID:AB_312727), IL-23R (clone 12B2B64, BV421, BioLegend, RRID:AB_2715804) were stained in staining buffer at a dilution of 1:200 on ice for 30 min, washed twice in staining buffer and then resuspended in 1 mL of fixation/permeabilization solution (Foxp3 Fix/Perm, ThermoFisher). After 45 min incubation on ice, samples were washed twice in staining buffer and then stained for intracellular markers IL-17A (clone eBiol7B7, APC, ThermoFisher), IL-10 (clone JES5–16E3, BV510, BD Biosciences), Foxp3 (clone FJK-16 s, FITC, ThermoFisher, RRID:AB_465243) and Rorγt (clone AFKJS-9, PE, ThermoFisher, RRID:AB_1834470) at a dilution of 1:100. Following 30 min of incubation, samples were again washed twice in staining buffer to be finally resuspended in 1 mL of staining buffer. Flow cytometry was conducted on the Attune NxT (ThermoFisher) and data analyzed using FCSExpress Research (v7.0).

2.11. Mammalian cell lines

The human adenocarcinoma Caco-2 cell line was procured from ATCC (HTB-37), derived from a 72 year old male Caucasian. Caco-2 cells were cultured in MEM media supplemented with 20% fetal bovine serum (FBS), glutamine (2 mM), penicillin/streptomycin antibiotics, sodium pyruvate (1 mM), sodium bicarbonate (1.5 g/L), and MEM non-essential amino acids (MEAAs) in T-25 adherent plates in 5% carbon dioxide atmosphere at 37 °C. To subculture cells, adherent cells were detached by aspirating media, washing once in sterile PBS and detaching cells using Trypsin-EDTA for 5 min. Cells were

gently tapped to dislodge, resuspended in 15 mL of reconstituted media and centrifuged for 8 min at 800 rpm. Cells were passaged every 2–3 days at a dilution factor of 1:4 into subsequent dishes. The human monocyte THP-1 cell line was procured from ATCC (TIB-202) from an infant male with acute monocytic leukemia. THP-1 cells were maintained in RPMI media supplemented with FBS (10%), penicillin/streptomycin antibiotics, beta-mercaptoethanol (0.05%) and sodium pyruvate (1 mM) in T-75 non-adherent plates in a 5% carbon dioxide atmosphere at 37 °C. To subculture cells, the suspension cells were collected and centrifuged at 800 rpm for 8 min. Cells were passaged every 3–4 days at a dilution factor of 1:6 into subsequent dishes.

2.12. In vitro cell culture model

To model the intestinal epithelial-immune cell interaction, a molecular bilayer of differentiated Caco-2 cells (apical layer) and differentiated THP1 monocytes (basolateral layer) was constructed on a transwell membrane plate (8 μm, Sigma). Before assembly of the bilayer, Caco-2 cells were cultured in MEM media (ThermoFisher) in 20% FBS, 5% penicillin/streptomycin solution supplemented with sodium pyruvate, sodium bicarbonate and MEAAs. At day 0, Caco-2 cells were seeded onto the transwell plates (12-well, 8 μm) at a concentration of 5×10^5 cells/well. The cells were allowed to polarize for 18 days until the TEER reached 500 ohmxcm^2 changing the media every 2–3 days. Likewise, THP-1 cultures were maintained as suspension cultures until 2 days before coculture assembly. THP-1 cells were differentiated into macrophages with phorbol 12-myristate 13-acetate (PMA, 15 nM) treatment for 48 h in a T-25 at a concentration of 3×10^6 cells/flask so that they became adherent. 24 h before assembly of the co-culture both the THP1 and Caco-2 cells were pretreated with either the BDPP, probiotic- or synbiotic-metabolites. Total BDPP, probiotic or synbiotic cultures were created by a 24 h fermentation in MRS-cysteine media, centrifuged, media collection of supernatant which was pH normalized to 7.4, filter sterilized and supplemented into the media at a dose of 50 μL/1 mL media. Individual metabolites were dosed as described in the individual experiments. To assemble the cocultures, 48 h PMA pre-treated differentiated THP1 cells were seeded on the bottom of a clean 12-well plate (1.8×10^5 cells/well) in the complete RPMI media without β-mercaptoethanol and allowed to attach for 2 h. The pre-treated differentiated Caco-2 cells on the transwell membrane were positioned atop the THP1 cell layer, and the metabolite supplements were reapplied along with L-tryptophan (10μg/mL media). To simulate an immune challenge, IFN-γ (10 μg/ml), LPS (1 μg/ml) and ATP were added to both the apical and basolateral compartments for 18 h. Before and after the 18 h incubation, TEER was recorded. Supernatant from both the apical and basolateral layers were collected, and cells were immediately rinsed in PBS and RNA extracted immediately using the Qiagen RNeasy kit. RNA and supernatant were stored at −80 °C until use. Primer sequences for the human genes are listed in Table S5.

2.13. Ethics statement

All procedures, protocols and behavioral experiments were approved by the Mount Sinai Institutional Animal Care and Use Committee (IACUC).

2.14. Statistical analysis

Details of individual experiments' statistical data can be found in figure legends. For behavior, gene and protein comparisons, statistical analyses were performed with a 2-way ANOVA and Tukey's post hoc multiple comparisons analyses. Summary of the F-statistics for the main effects and interactions can be found in Table S6. Behavioral experiments were completed with $n = 12–16$ animals as described in the method details whereas all gene and protein analyses were conducted with an $n = 6$ representing individual mice. Flow cytometry was conducted with $n = 3$ independent mice with statistical significance between samples calculated with the student's *t*-test. In all cases, significance was determined as $p < 0.05$. Nanostring multiplexing samples were conducted with $n = 3$ independent samples with all analyses conducted with the nCounter software. All other statistical analyses were conducted in GraphPad Prism version 8.0.

3. Results

3.1. A synbiotic increases plasma and brain bioavailability of microbial-derived phenolic metabolites

The synbiotic used in this study combines the probiotics *Lactobacillus plantarum* ATCC 793 and *Bifidobacterium longum* ATCC 15,707 with a Bioactive Dietary Polyphenol Preparation (BDPP) composed of 1% *w/v* grape seed polyphenol extract, 1% *w/v* resveratrol and a 5% *w/v* concord grape extract. The ability of chronic synbiotic administration to alter the bioavailability of BDPP polyphenols and the derived metabolites in the plasma and brain was assessed through pharmacokinetics studies conducted over a period of 24 h and directly compared to the chronic administration of BDPP alone. Results are summarized in Table 1 and we have excluded some undetectable phenolics from the 44 compounds surveyed. In plasma, synbiotic treatment effectively elevated the area under the curve (AUC) of several phenolic acid metabolites including gallic acid (GA), 4-hydroxycinnamic acid (4-HCA), homovanillic acid (HVA), 3-hydroxyphenylpropionic acid (3-HPPA), 4-HPPA, 3-hydroxyphenylacetic acid (3-HPAA), the resveratrol microbial metabolite dihydroresveratrol (DHRSV), and the characteristic flavonoid microbial metabolite 5-(3′,4′-dihydroxyphenyl)-γ-valerolactone (DHVL) (Ottaviani et al., 2018), and some polyphenol precursors including epicatechin (EC) as well as its methyl ester (Me-EC), and all the flavonols evaluated, i.e., kaempferol (KAMF), quercetin (QUER), isohamnetin (3′-MeQ), rhamnetin (7′-MeQ) and myricetin (MYR) (Table 1). Yet, BDPP administration alone resulted in higher plasma levels of the phenolic acid metabolites 3-hydroxybenzoic acid (3-HBA) 3,4-dihydroxybenzoic acid (3,4-diHBA), vanillic acid (VA), ferulic acid (FA) and 3,4-dihydroxyphenylacetic acid (3,4-diHPAA). There were also higher levels of some polyphenol precursors including resveratrol (RSV), catechin (C) and its methyl ester (Me-C) indicating the different metabolic potential and catabolic preference of mice chronically administered to a synbiotic over a polyphenolic formula without probiotics addition. Some of these distinct pharmacokinetics features we found in plasma were propagated into the brain. Despite the BDPP-only treated group having higher levels of 3,4-diHBA and 3,4-diHPAA in the plasma, the synbiotic-treated group demonstrated higher levels of all the hydroxybenzoic acids and mono-hydroxyacetic acids surveyed in the brain. Additionally, the synbiotic treatment appears to promote the

methylation of quercetin and subsequent elevation in the deposition of 3′-MeQ and 7′-MeQ in the brain compared to the BDPP-only group (Table 1).

The pharmacokinetics following both chronic BDPP and synbiotic treatment is displayed as the maximum concentration reached at what time after the bolus dose (C_{max}) and the area under the curve (AUC). Statistical variations in the AUC between the BDPP and synbiotic groups are shown with the asterisk beside the higher value. Each value has $n = 6$ +/− SEM with *$p < 0.05$, **$p < 0.01$. Gallic acid (GA), Pyrogallol (PG), 4-Hydroxyhippuric acid (4-HHA), Delphinidin-3-O-glucoside (D3Glc), 3,4-Dihydroxybenzoic acid (3,4-diHBA), 3-Hydroxyhippuric acid (3-HHA), 3,4-Dihydroxyphenylacetic acid (3,4-diHPAA), 4-O-Methylgallic acid (4-MeGA), Cyanidin-3-glucoside (C3Glc), 4-Hydroxybenzoic acid (4-HBA), Catechin (C), Hippuric acid (HA), Malvidin (Mvd), 4-Hydroxyphenylacetic acid (4-HPAA), 3-(3,4-Dihydroxyphenyl)propionic acid (3,4-diHPPA), Vanillic acid (VA), Malvidin-3-glucoside (M3Glc), Caffeic acid (CA), O-Methyl catechin (Me-C), 3-Hydroxybenzoic acid (3-HBA), Proanthocyanidin dimer B2 (PAC-B2), 3-Hydroxyphenylacetic acid (3-HPAA), Homovanillic acid (HVA), Malvidin (Malv), Epicatechin (EC), 5-(3′,4′-Dihydroxyphenyl)-γ-valerolactone (DHVL), 3-(4-Hydroxyphenyl)propionic acid (4-HPPA), 4-Hydroxycinnamic acid (4-HCA), O-Methyl epicatechin (Me-EC), Dihyroferulic acid (DHFA), 3-(3-Hydroxyphenyl)propionic acid (3-HPPA), Ferulic acid (FA), 3-Hydroxycinnamic acid (3-HCA), Phenylacetic acid (PA), 5-(3,4-Dihydroxyphenyl)valeric acid (3,4-diHPVA), Myricetin (MYR), t-Resveratrol (−) (RSV), Dihydroresveratrol (DHRSV), 5-(4-Hydroxyphenyl)valeric acid (4-HPVA), 5-(3-Hydroxyphenyl)valeric acid (3-HPVA), Quercetin (QUER), Kaempferol (KAMF), Isorhamnetin (3′-MeQUER), Rhamnetin (7-MeQUER).

3.2. Stress-Induced depressive- and anxiety-like behaviors are ameliorated by synbiotic treatment

Following 28 days of chronic unpredictable stress (CUS; Fig. 1a), stressed controls exhibited significant depressive- and anxiety-like behaviors compared to unstressed vehicle controls. In the open field test for anxiety-like behavior, stressed controls exhibited reduced time in the center zone compared to vehicle controls, which was improved by BDPP- and synbiotic-, but not probiotic-treatment with respect to stressed controls. Likewise, both BDPP and synbiotic treatment rescued the anxiety-like phenotype in response to stress (Fig. 1b). There were no variations in immobilization time between the non-stressed treated groups following the forced swim test (FST) protocol for depressive-like behavior; however, stressed controls and BDPP-treated mice had increased immobilization time compared to their non-stressed controls indicating an increase indepressive-like behavior. Both probiotic- and synbiotic treatment rescued the depressive-like behavior compared to their unstressed controls, while the BDPP-, probiotic- and synbiotic-treated groups all had reduced immobilization times compared to the stressed-controls (Fig. 1c).

3.3. A synbiotic rescues stress-induced reduction in serotonin through inflammatory and kynurenine pathway regulation

Serotonin, a neurotransmitter implicated in neuropsychiatric disorders, is regulated by the gut microbiota (Camilleri, 2009). In plasma, serotonin remained unchanged despite stress or

treatment (Fig. 2a). In the prefrontal cortex, stress reduced serotonin production in vehicle controls, an effect that was rescued only by synbiotic treatment. Similarly in the ileum, stress reduced serotonin in vehicle controls and probiotic-treated mice, which was rescued by the synbiotic (Fig. 2a). Serotonin reduction reflects the redistribution of its precursor tryptophan towards kynurenine pathway metabolism, occurring under conditions of inflammation, generating neuroprotective (kynurenic acid) and neurotoxic (QA) metabolites. Supporting this, elevated QA was found in the serum of stressed vehicle controls, rescued by all treatments but reduced specifically by the synbiotic (Fig. 2b). The rate-limiting step of kynurenine pathway metabolism is activation of tryptophan-2,3-dioxygenase (TDO) in the liver and indoleamine-2,3-dioxygenase (IDO) in immune cells, epithelial cells and other tissues by proinflammatory mediators including interferon (IFN)γ. *Ido* mRNA expression was elevated in the prefrontal cortex, hippocampus, liver and most strongly in the ileum of stressed vehicle controls (Fig. 2c). In the ileum, treatment with probiotic and synbiotic eliminated the stress-induced induction of *Ido*, whereas in the prefrontal cortex, no treatment effects were observed (Fig. 2c). In both the liver and hippocampus, the stress-induced increase in *Ido* was reduced by the synbiotic and in all tissues, BDPP had no beneficial effect. Kynurenine-3-monooxygenase (KMO) converts kynurenine into 3-hydroxykynurenine promoting the production of QA. *Kmo* mRNA expression in the prefrontal cortex was significantly elevated by stress in the control group, yet unaffected by treatment. In the liver, the stress-induced increase in *KMO* was reduced only by the synbiotic (Fig. 2d), demonstrating a tissue-specific regulation of kynurenine pathway enzymes. Gene expression of other kynurenine pathway genes including quinolinic acid phosphoribosyltransferase, 3-hydroxyantranilic acid dioxygenase, and kynureninase was not significantly impacted by stress or treatment groups (data not shown).

3.4. Stress-induced peripheral and neuroinflammatory responses are attenuated by a synbiotic

The regulation of IDO and kynurenine pathway metabolism is tightly linked to the inflammatory milieu in both the periphery and the brain. In addition, the peripheral immune status influences neuroinflammation as immunomodulators can cross the BBB stimulating microglia and the consequent neuroinflammatory reactions (Chavan et al., 2017). To assess whether stress-induced neuroinflammation occurs independent or consequent of the peripheral immune status, immune activators were assessed in the brain and periphery. IL-1β was significantly upregulated in the serum, prefrontal cortex, hippocampus, cortex and ileum of vehicle control stressed mice, while the symbiotic reduced IL-1β levels in all tissues tested. Likewise, probiotic treatment reduced stress-induced IL-1β levels in the prefrontal cortex, hippocampus and cortex while BDPP reduced IL-1β in the prefrontal cortex only (Fig. S2a). IL-6 had a stronger response to stress in the periphery compared to the brain with potent upregulation in the serum, liver and ileum, all of which were reduced by synbiotic treatment. - There was a slight stress-induced increase of IL-6 in the hippocampus, but this was unaffected by treatment (Fig. S2b).

To decipher what is driving the variations in cytokine expression in the brain and periphery and to relate this to serotonin levels, expression of a battery of sterile and canonical inflammatory signaling cascade molecules was assessed by real-time PCR and presented as

a heatmap of the ratio of stressed vs. non-stressed groups within the respective treatment group (Fig. 2e). Toll-like receptor (*Tlr4*) expression was upregulated in the stressed controls' brain regions, but more highly in the ileum indicating that some GI-derived pathogen associated molecular patterns (PAMPs) may by driving the IL-1β and IL-6 responses in the periphery. Likewise, a significant upregulation of *NfkB*, *Il-6* and *Il-1β* mRNA was observed in the ileum of stressed controls, all of which were significantly downregulated by the various treatment groups. In contrast, in all brain regions, weaker and less consistent inductions of *Tlr2/4* and *NfkB* signaling as well as downstream *Il-6* responses were observed; however, there was a strong upregulation of *Nlrp3* mRNA expression, its activator *Hmgb1,* receptor *P2X7* and downstream effectors *Il-1β*, *Il-18* and *Casp1*.This dichotomy suggests that in the periphery, the canonical inflammatory cascades are being activated driving a strong release of the proinflammatory cytokines IL-6 and IL-1β while in the brain, possibly consequent of the peripheral immune activation, a sterile inflammatory response implicating the NLRP3 inflammasome is being stimulated. Importantly, treatment with the synbiotic and its specific arsenal of plasma- and brain-bioavailable metabolites effectively downregulated both the peripheral and brain proinflammatory response to stress, to a greater extent than BDPP or probiotic treatment alone.

3.5. Immune cell recruitment and aryl hydrocarbon receptor activation may drive the synbiotic-Induced changes in the inflammatory response to stress

To elucidate the dichotomy of inflammatory responses in the periphery and the brain, NanoString multiplex counting was used. Generally, stress upregulated proinflammatory and downregulated anti-inflammatory genes in the prefrontal cortex, hippocampus, liver and ileum while treatment with BDPP, probiotics or synbiotics induced the opposite effect, but to different proportions depending on the treatment and tissue (see attached excel file). Gene expression variation was calculated as the relative gene expression of each stressed-treated group compared to the unstressed vehicle control. Using this comparative data, specific pathway-related effects of the different treatments were assessed using Qiagen's Ingenuity Pathway Analysis (IPA) and the canonical pathway expression score is displayed as a heatmap. In the prefrontal cortex, the canonical signaling pathways upregulated in stressed controls include death receptor signaling, neuroinflammation, IL-22, HMGB1, IL-1, IL-18 and to a lesser extent, inflammasome and immune cell signaling pathways (Fig. 3a). Assessing the overall neuroinflammatory pathway in stressed controls, altered HMGB1 signaling through upregulated TLR4 receptor expression is driving the downstream neuroinflammatory phenotype including cytokine upregulation, neuronal damage and BBB disruption (Fig. S3). This pathway also suggests that stress stimulates T cell recruitment via ICAM, VCAM, CCL5 and CXCL8. Supporting this, TWEAK signaling, upregulated by stress, induces transcription of immune cell recruitment molecules such as MMP9, VCAM and CCL2, was downregulated by all treatment groups. qPCR analysis confirmed that mRNA expression of *Ccl2*, *Ccl5*, *Icam* and *Vcam*, controlling various aspects of immune cell chemotaxis, were upregulated in the stressed controls, and downregulated by synbiotic treatment (Table S7). While there was little overall effect of BDPP treatment in the prefrontal cortex on any of the neuroinflammatory marks, the synbiotic downregulated all of the affected pathways including neuroinflammatory, IL-1, IL-22 and IL-18 signaling while additionally, downregulating dendritic cell maturation, IL-6, MAPK and IL-7 signaling

pathways. Other upregulated pathways of interest (not shown) include the insulin receptor signaling pathway, which is associated with cognitive decline (Han et al., 2016) and IRF signaling, which is the master regulator of TLR signaling cascades (Kawasaki and Kawai, 2014).

Similar effects of stress and synbiotic treatment were observed in the hippocampus (Fig. 3b). TNFR2, MIF regulation of innate immune, NF-κB and neuroinflammation pathways were highly upregulated in stressed controls, each which were downregulated only by synbiotic treatment. Synbiotic treatment also downregulated IL-6, TLR, IL-1, leukocyte extravasation signaling and T cell and dendritic cell signaling pathways, albeit little change was observed in the stressed controls. BDPP treated elicited little impact on hippocampal signaling while probiotic treatment trended towards an upregulation of neuroinflammatory pathways including IL-6, STAT3, TLR, IL-1 and T and dendritic cell signaling. Upregulation of phagocyte migration in stressed controls along with phagocytosis and differentiation of T lymphocytes was also observed using regulatory pathway predictions (Fig. S4a,b). Likewise, synbiotic treatment in the hippocampus downregulated the neuroinflammatory signaling pathways with predicted downregulation of lymphocyte movement and phagocytosis (Fig. S4c), corresponding to the key canonical pathway variations.

In the liver, stress upregulated neuroinflammatory pathways, dendritic and CD28 signaling in T helper cells with mild effects on IL-6, HMGB1, macrophage reactive oxygen species (ROS) production and death receptor signaling (Fig. 3c). Synbiotic and probiotic treatment positively downregulated most of these pathways, while additionally downregulating NFAT regulation of the immune response, IL-8, NF-κB and B cell receptor signaling, demonstrating that the probiotic has a greater impact on peripheral immune markers than in the brain. Regarding overall pathway analysis, the reduction of NF-κB signaling in the liver by the synbiotic was the most important influence on reducing peripheral inflammatory activation due to stress (Fig. S5).

Of all the tissues studied, the most dramatic changes were observed in the ileum. In the stressed controls, there was a strong upregulation of NF-κB, P2Y purinergic receptor, inflammation, T and B cell signaling, Fc receptor-mediated phagocytosis in macrophages and monocytes, leukocyte extravasation signaling, AHR and TLR signaling, all of which were reduced by the probiotic, but to a greater extent, synbiotic treatment (Fig. 3d). Correspondingly, there was a downregulation of the T cell exhaustion pathway and antioxidant action, both reversed by probiotic and synbiotic treatment. This was confirmed by a synbiotic-induced decrease in *Ccl2, Icam* and *Vcam* mRNA expression by qPCR indicating that the synbiotic may be attenuating the inflammatory response by controlling the infiltration of immune cells into the GI tract (Table S6). Using IPA's disease functionality assessment, the major disease-risk pathways that were upregulated due to stress where neurological disease, GI tract inflammation and the general inflammatory response. Assessing predicted regulatory pathways, one transcription factor, the AHR, was identified as being significantly upregulated in the synbiotic-treated stressed mice contributing broadly to the synbiotic's anti-inflammatory and protective actions. The AHR responds to environmental cues and facilitates the reprogramming of naïve immune cells including monocytes and lymphocytes. In the ileum, upregulation of the AHR by the synbiotic had

predicted effects on downregulating morbidity and inflammation, ultimately leading to enhanced survival (Fig. S6). Verifying this association with qPCR, there was no upregulation of *Ahr* mRNA expression in any of the tissues in response to stress; however, *Cyp1a1*, an immediate downstream target, was upregulated solely in the ileum by synbiotic treatment validating AHR's functional activation (Table S6).

3.6. A synbiotic ameliorates the stress-Induced increase of the T helper 17 to regulatory T cell ratio

The AHR is a critical component of lymphocytes' response to the immune-modulating environmental cues from the GI tract, including gut microbiota-derived metabolic products (Lamas et al., 2018). AHR signaling modulates the transition between proinflammatory T helper (Th)17 cells and immunomodulatory regulatory T cells (Tregs) by both influencing the transcriptional profile of the naïve lymphocytes and altering the inflammatory milieu generated by innate immune cells (Gutiérrez-Vázquez and Quintana, 2018). Based on the predictive correlation between AHR upregulation by the synbiotic and the downregulation of immune cell signaling, the implications of the synbiotic on the Th17 to Treg ratio in the context of stress was investigated. The ratio of IL-17A to IL-10 is a broad indication of the activity of Th17 vs. Tregs. In both the serum and ileum, the ratio of IL-17A to IL-10 was elevated 2.0- and 1.5-fold, respectively, in response to stress (Fig. 4a). In serum, both probiotic and synbiotic treatment reduced this ratio, while in the ileum, only the synbiotic elicited an active reduction, which was significantly less than any of the other treatment groups. Investigating cellular activation at a higher level, gene expression of *Foxp3*, the activator of Treg development, *Rorγt* for Th17 expression, *Tbet* and *Gata3*, leading to Th1 and Th2 cell types, respectively was determined (Fig. 4b). In the ileum and liver, there was a strong upregulation of all the T cell transcription factors in response to stress, with a potent downregulation by both probiotic and synbiotic. In unstressed controls in the ileum, the synbiotic increased *Foxp3* expression by 8.7 +/− 0.2 fold ($p < 0.05$), which was higher than the increase implemented by both the probiotic (4.1 +/− 0.3, $p < 0.05$) and BDPP (3.55 +/− 0.2, $p < 0.05$). Likewise, in response to stress, there was a 2.3 +/− 0.2 ($p < 0.05$) fold increase in *Rorγt* expression in controls, which was significantly reduced by both the probiotic (1.1 +/− 0.2, $p < 0.05$) and the synbiotic (1.1 +/− 0.1, $p < 0.05$). Most importantly, the ratio of *Foxp3* to *Rorγt* expression in the ileum of stressed mice was decreased to 0.28 +/− 0.08 fold ($p < 0.05$) in controls, but increased only by the synbiotic (1.3 +/− 0.2, $p < 0.01$) suggesting that in the ileum, the synbiotic uniquely upregulates the Treg/Th17 ratio in response to stress. These strong variations were not observed in the liver or brain tissues and variations in the *Gata3/Tbet* ratio in the ileum and other tissues were highly variable, without clear distinctions between treatment groups. Activation markers of both Tregs (*Il-10*) and Th17 cells (*Il-23R, Il-17A*) were also positively impacted by the probiotic and the synbiotic in the ileum and liver suggesting that not only the quantity of cell types are being altered, but also their activation state in response to stress.

Th17 and Tregs are not distinct populations, but rather exist along of spectrum that can be shifted depending on the inflammatory microenvironment (Diller et al., 2016) making gene expression analyses insufficient. To decipher the differential cell populations, flow cytometry analyses of $CD3^+$ $CD4^+$ lymphocytes for $ROR\gamma t^+$ (Th17) and $Foxp3^+$

populations (Treg) was conducted including the activated cell types characterized as IL-17A$^+$ IL23R$^+$ or IL-10$^+$ activated cells, respectively. Based on the invariability of the gene and cytokine data in the unstressed treated groups, all stressed treated groups were compared to the unstressed vehicle control. In the serum, there were no significant differences in the Treg/Th17 cell ratio, or the activated cell populations (Fig. 4c,d). In the liver, there were again no changes in the ratio of cell populations; but, there was a decrease in activated Treg/Th17 cells in controls, which was reversed by synbiotic treatment (Fig. 4e,f). In the ileum, a stark decrease in both cell and activated cell populations of the Treg/Th17 was observed, again ameliorated only by synbiotic treatment (Fig. 4g,h) suggesting that the synbiotic is attenuating the stress-induced adaptive immune response by altering the ratio of Treg/Th17 cells.

3.7. Exogenous AHR inhibition in vitro blocks the synbiotic's metabolites anti-inflammatory activity

The AHR has many gut-derived endogenous ligands including polyphenolic flavonoids, indoles and tryptophan metabolites (Nguyen and Bradfield, 2008). To test if synbiotic-derived polyphenolic metabolites, as determined with the bioavailability study, attenuate the inflammatory response of macrophages through the AHR, a coculture of human adenocarcinoma cells (Caco-2) and activated macrophages (THP-1) was constructed to model the gut epithelial-immune cell interaction. Inflammation was modelled as a low-dose LPS challenge in which untreated controls exhibited a decrease in epithelial integrity measured as the transepithelial electrical resistance (TEER) and an increase in cytotoxicity, kynurenine production and IL-1β production (Table 2). To test which plasma synbiotic-derived metabolites (Table 1) were conveying the synbiotic's anti-inflammatory activity, two concentrations of several metabolites were tested in the LPS-treated coculture system (Table S8). Based on the metabolite's effects on TEER, cytotoxicity and the induction of kynurenine and *Il-1β* gene expression, it was determined that the best candidates for AHR-specific signaling included 4-HPAA, 4-HPPA, CA, 3′MeQ, 7′MeQ and Kamf, as these metabolites invoked dose-dependent anti-inflammatory effects, which correlated to *Cyp1a1* mRNA expression (Table S8). To test the direct effect of AHR signaling, cells were pretreated with an AHR antagonist 6, 2, 4′-trimethoxyflavone (TMF) before the LPS challenge, which was confirmed to reduce AHR activity with reduced *Cyp1a1* expression. TMF inhibited the synbiotic's ability to increase TEER, reduce cytotoxicity and ameliorate kynurenine and IL-1β production in response to LPS challenge (Table 2). In addition, the beneficial effects of 4HPAA, 4HPPA and CA were similarly abrogated by TMF whereas the anti-inflammatory activity of 3′MeQ, 7′MeQ and Kamf occurred independent of AHR signaling. In THP-1 cells, TMF reversed the synbiotic's beneficial effect on *Nlrp3, Casp1, IL-10* and *Icam* mRNA expression. Similar trends were observed for the 4HPPA, 4HPAA and CA metabolites with the flavanols being less affected by TMF treatment. Interestingly, *Tlr4* expression was suppressed in TMF-treated synbiotic, 4HPAA, 4HPPA and CA while in the flavanol-treated culture, *Tlr4* was strongly upregulated (Fig. 5a). In Caco-2 cells, AHR signaling observed through *Cyp1a1* expression was strongly downregulated by TMF as expected, with a general decrease in the tight junction protein zona occludin (*Zo1*), claudin (*Clnd*) and occludin (*Occ*) across all treatment groups (Fig. 5b). This shows that the impact of AHR signaling is specific to THP-1 cells and only specific synbiotic-derived metabolites

4HPAA, 4HPPA and CA indicating a putative mechanisms of synbiotic-induced variations in the Treg/Th17 ratio in response to stress.

Cocultures of human colorectal adenocarcinoma (Caco-2) and phorbyl 12-myristate 13-acetate (PMA)-activated human monocyte (THP1) cells were pretreated with the supernatant of 24 h fermented BDPP, probiotic or synbiotic solutions or specific metabolites (250 ng/mL) for 24 h before stimulation with LPS, IFNτ and ATP for 8 h. Wells were also treated with or without 6, 2, 4′-trimethoxyflavone (TMF), a potent AHR antagonist. Treatment- and TMF-induced variations in transepithelial electrical resistance (TEER), cytotoxity measured with an lactate dehydrogenase (LDH) release assay, kynurenine with a chemical assay and IL-1β with ELISA. TEER, cytotoxicity and kynurenine are represented as percentage of control while IL-1β is fold change from untreated controls. Each sample has $n = 4$ independent samples mean +/− SEM, significance calculated with a student's t-test *$p <$ 0.05, **$p < 0.01$ within the same treatment group and τ $p < 0.05$ compared to LPS-treated control (highlighted in grey).

4. Discussion

Probiotics and gut microbiota-derived metabolites play a significant role in managing cognition and mood, especially under conditions of chronic stress (Burokas et al., 2017; Liang et al., 2015). Indeed, gut-brain-axis mechanisms, including inflammation, the regulation of neurotransmitters and their precursors are linked to the development of stress-induced neuropsychiatric conditions (Strandwitz, 2018; Clark and Mach, 2016; Petra et al., 2015). Synbiotics provide a useful therapeutic strategy over conventional treatments for neuropsychiatric disorders as synbiotics inherently address the diseases' multifactorial nature through the generation of a battery of bioactive metabolites. The stress-induced physiological adaptations characteristic of depression include neurodegeneration, impairment of hippocampal neurogenesis, reduced serotonergic signaling, altered HPA axis regulation and importantly, modulated neuro- and peripheral-inflammatory processes (reviewed in (Mahar et al., 2014). A handful of clinical trials have established efficacy for the use of probiotics and synbiotics against depression (Vaghef-Mehrabany et al., 2019) including one recent study where synbiotic treatment to 75 hemodialysis patients over twelve weeks resulted in greater improvement of depressive scores and serum brain-derived neurotropic factor (BDNF) levels compared to probiotic treatment alone (Haghighat et al., 2019). Here, BDPP attenuated while the probiotic and synbiotic treatment eradicated depressive-like behavior as observed by immobilization time in the forced swim test. In contrast, stress-induced anxiety-like behavior observed as time in a center compartment of the open field test was improved by both synbiotic and BDPP treatment demonstrating how the synbiotic consistently attenuates diverse stress-induced behaviors. This feature can be attributed to the increased bioavailability and bioactivity of the synbiotic-derived metabolites. The synbiotic generated a larger host of plasma- and brain-bioavailable metabolites than BDPP alone as the synbiotic includes probiotic bacteria that are responsible for the fermentation of the parent polyphenols present in BDPP. In addition, the probiotics and polyphenolic prebiotic together alter the composition of the gut microbiota differently than the prebiotic alone creating a bacterial environment that is more efficient at cross-feeding and consequently, metabolite production (Gurry, 2017). As indicated previously, the

behavioral outputs observed here can only be generalized for male mice, as female mice respond different to stress. Further, these behavioral test have limitations (Hodes et al., 2015). The forced swim test only measures one dimension of depression, anhedonia, while human depression is multifaceted so conclusions can only be reared on this symptom of depression (Bourin et al., 2001). The sucrose preference test was intentionally not used in this study as the BDPP and probiotic solutions have a slight flavor, which could confound the taste test. Similarly for the open field test, the center measure represents only one aspect of anxiety and cannot be generalized to the complexity of the human condition (Seibenhener and Wooten, 2015). Nevertheless, both the forced swim and open field tests are robust, well characterized test that together validate how the synbiotic can attenuate the chronic stress associated behaviors.

4.1. A synbiotic regulates serotonin availability through the kynurenine pathway

Of the body's serotonin, 95% is located in the GI tract (Camilleri, 2009) and the gut microbiota heavily influences the metabolic fate of tryptophan by modulating the local inflammatory milieu (O'Mahony et al., 2015). The balance of tryptophan metabolism towards either kynurenine or serotonin production depends on the expression of ubiquitously distributed IDO and hepatic TDO (Clarke et al., 2012). IDO activity is stimulated by the cytokines IFNγ, TNFα and IL-1β while TDO is induced by glucocorticoid release: both characteristics of stress-induced depression. Thus, it would be expected that IDO and TDO expression would be upregulated under conditions of chronic stress consequently reducing serotonin and increasing kynurenine metabolite production.

The stress-induced reduction of serotonin in the prefrontal cortex and the ileum was rectified only by the synbiotic demonstrating a direct correlation between serotonin metabolism in the GI tract and the brain. There was a disparate relationship between treatment group and tissue-specific expression of *Ido*. *Ido* mRNA expression was ubiquitously elevated in the brain and periphery in response to stress, and the synbiotic effectively downregulated its expression in the hippocampus, liver and most significantly in the ileum. However, probiotic treatment also downregulated *Ido* expression in the ileum and hippocampus, which does not correspond to the serotonin levels in either the ileum or the prefrontal cortex. Serotonin levels are impacted by many gut-derived factors. Gut microbiota metabolites including the short chain fatty acids (SCFAs) downregulate IDO activity in intestinal epithelial cells by modulating IFNγ release (Martin-Gallausiaux et al., 2018). Gut-derived tryptophan metabolites including indoles can alter expression of kynurenine pathway enzymes including KMO and QPRT, which subsequently alter local serotonin levels (Waclawiková and El Aidy, 2018). Finally, local IDO expression in monocytes and microglia (Schulz et al., 2015) may be impacted by the synbiotic-specific BBB-permeable metabolites, and not by the probiotic-derived metabolites also influencing local production of serotonin.

Serotonin levels and the synbiotic's beneficial effects directly correlated to QA levels in the serum (Stone et al., 2013). Elevated QA occurs in both the serum and cerebral spinal fluid of patients with neurodegenerative and inflammatory disorders, including depression (Steiner et al., 2011; Savitz, 2017) and is strongly correlated to depressive suicidal victims (Brundin et al., 2016). The rate limiting step for the production of QA is the activation of KMO, an

enzyme highly expressed in microglia, monocytes and macrophages (Jones et al., 2015) and inhibition of KMO with natural polyphenols is neuroprotective (Zhang et al., 2019). In the present study, *KMO* mRNA expression was elevated in the prefrontal cortex in response to stress, and its expression normalized by BDPP, probiotic and synbiotic treatment. In the liver, the stress-induced elevation of *KMO* was reduced only by the synbiotic whereas in the ileum, there were neither stress- nor treatment-related effects. Compared to serotonin, QA corresponded more closely to the treatment-dependent effects on stress-induced behavioral abnormalities and may act as a more accurate biomarker. Despite these multiple mechanisms regulating IDO activity and the fate of tryptophan metabolism, the common link is the inflammatory milieu, both in the periphery and the brain.

4.2. Stress, neuroinflammation and depression

Stress promotes neuroinflammation precipitating the symptoms of depression (rev. in (Kim and Won, 2017). Although glucocorticoids are generally anti-inflammatory, chronic glucocorticoid elevation has proinflammatory effects in the brain (Dinkel et al., 2003) in a manner dependent on NF-κB induction (Munhoz et al., 2010), which is important for the stress-induced depressive-like behaviors in mice (Koo et al., 2010). Peripheral inflammation is also an essential component of stress-induced depression. Depressed individuals have elevated circulating monocytes and proinflammatory cytokines including IL-1β, TNF-α and IL-6 (Dowlati et al., 2010; Howren et al., 2009), leading to elevated macrophage infiltration into the perivascular space and consequent microglia activation (Torres-Platas et al., 2014). This creates a positive feedback loop were peripheral inflammation drives microglial ramification and activation (D'Mello et al., 2009), elevated production of cytokines and chemokines in specific corticolimbic brain regions (Walker et al., 2014), stimulating infiltration of monocytes into those regions further exasperating the neuroinflammatory phenotype implicated in the development and recurrence of anxiety- and depressive-like behavior (Wohleb et al., 2014).

In the current study, IL-1β was ubiquitously upregulated by stress in all regions investigated. The most dramatic changes occurred in the ileum, serum and prefrontal cortex, supporting the importance of the prefrontal cortex in depression's behavioral deficits (Seo et al., 2017; Belleau et al., 2019). In contrast, IL-6 was only upregulated in the periphery in response to stress. Importantly, stress-induced IL-1β or IL-6 upregulation in any region, was abrogated by the synbiotic whereas BDPP and probiotic treatments had tissue- and cytokine-specific effects. Further, the proinflammatory profiles in the brain were not consistent with the behavioral data indicating that there are deeper levels of regulation impacting the gut-brain-axis-mediated biobehavioral responses to stress. This also indicates that immune regulation in the periphery and the brain are different and it is possible that the proinflammatory state in the periphery is influencing neuroinflammation. Similar peripheral-central innate immune crosstalk has been proposed for systemic lupus erythematosus (Tomita et al., 2004), Parkinson's disease (Fuzzati-Armentero et al., 2019) and Alzheimer's disease (Park et al., 2019; Dionisio-Santos et al., 2019) and the remainder of this study aimed to detangle this crosstalk and understand the specific inflammatory mechanisms responsible for the gut-brain-axis-derived influence on the peripheral-central immune crosstalk in the context of stress-induced depression.

4.3. Peripheral-Central immune crosstalk drives Stress-Induced depression

The immune status of the periphery directly impacts the inflammatory state of the brain driving neuropathologies (Kempuraj et al., 2017). To tease apart the disparate effects of neuroinflammation and behavioral phenotypes, a mRNA expression analysis of typical inflammatory elements was conducted. The immune regulation was highly tissue-specific. The canonical inflammatory pathways TLR2/4 to NF-κB signaling were more highly upregulated in the ileum compared to the brain. One group reported that chronic stress could be prevented by blocking TLR4 activity in the prefrontal cortex (Wang et al., 2018); however, the TLR4 inhibitor was injected interperitoneally indicating that the blocked TLR4 response may have been occurring in the periphery, propagating the effect into the brain. In contrast, upregulation of the NLRP3 inflammasome pathway mediators including HMGB1, P2X7 and the downstream factors IL-18 and Casp1, were comparatively enriched in the brain.

NLRP3 inflammasome signaling is an orchestrator of the neuroinflammatory response to depression (Herman and Pasinetti, 2018), whereas in the GI tract, the impact of NLRP3 activation on neuroinflammation is less well defined. Pharmacological inhibition of the NLRP3 inflammasome attenuated depressive-like behaviors in a similar 28 day CUS protocol (Zhang et al., 2015); however, these effects are likely primarily through neuroinflammatory responses. In the GI tract, NLRP3 activation contributes to elevated IL-1β in inflammatory bowel disease (Mao et al., 2018). In a colitis model, *Nlrp3*$^{-/-}$ mice have an increased frequency of tolerogenic CD103^{+} dendritic cells, lower Th17 immunity and a reduced colitis phenotype, however unchanged expression of IL-18 suggested that these effects could be independent of NLRP3 signaling (Mak'Anyengo et al., 2018). This is in line with the observation that resident colonic macrophages are hyporesponsive to NLRP3 inflammasome activation due to extensive post-transcriptional control of NLRP3 and pro-IL-1β through the ubiquitin/proteasome system (Filardy et al., 2016).

Using NanoString neuroimmune profiling, it was confirmed that the overall neuroinflammatory state of the prefrontal cortex, hippocampus, liver and ileum was upregulated in response to stress with the synbiotic consistently reducing the inflammation compared to the tissue-specific effects of the probiotic and BDPP. In addition, distinct tissue-specific canonical pathways were shown to be associated to the inflammatory phenotypes. In the prefrontal cortex and hippocampus, the neuroinflammation was associated with NF-κB, inflammasome-mediated pathways and upregulation of innate immunity. In stark contrast, inflammation in the peripheral tissues correlated to the activation of peripheral immune cells including dendritic cells, macrophages, T helper cells, neutrophils and B cells. In the ileum, there was also stress-induced upregulation of leukocyte extravasation, iCOS-iCOSL and CD28 signaling indicating that leukocytes were being recruited to and activated in the GALT. It has been well characterized that chronic stress increases the infiltration of monocytes and dendritic cells into the brain (Wohleb et al., 2014) and this behavior mediates chronic stress-induced anxiety-like behavior (Wohleb et al., 2013), while stress hormones in response to acute and repeated stress orchestrate the redistribution of immune cells in the body in hormone- and tissue-dependent manners (Dhabhar et al., 2012). Importantly, stress-induced increase of immune cell recruitment to

the colonic lamina propria (Gao et al., 2018a, 2018b) and hematopoiesis (Yan et al., 2018) depend on the gut microbiota. The histone deacetylase activity of butyrate, one of the major SCFAs, can alter the expression of monocyte chemoattractant protein (MCP)1 and vascular adhesion molecule (VCAM)1 reducing the infiltration and migration of macrophages into the gut (Zapolska-Downar et al., 2004; Maa et al., 2010). In addition, butyrate can reduce proinflammatory chemokines and cytokines release from dendritic cells and monocytes modulating leukocyte trafficking (Gonçalves et al., 2018). A similar effect has been noted for several polyphenols including resveratrol (Cicha et al., 2011), GSPE in renal injury (Bao et al., 2015), the microbiota-derived flavan-3-ol metabolite 5-(3′,4′-dihydroxyphenyl)-γ-valerolactone (Lee et al., 2017) and others. Importantly, one study showed that metabolites of catechins and quercetin were more effective than their parent polyphenols at reducing monocyte adhesion to human aortic endothelial cells (Koga and Meydani, 2001), supporting the enhanced efficacy of synbiotic treatment at modulating monocyte recruitment and trafficking in the context of stress.

4.4. The synbiotic modulates activated lymphocyte ratios in response to stress through the AHR

Biochemical and flow cytometry analyses verified that the synbiotic reversed the stress-induced increase in the activated Th17/Treg ratio, validating the hypothesis driven by the NanoString data. RORγt^+ Th17 and Foxp3$^+$ Tregs are the most abundant lymphocytes in the lamina propria (Maloy and Kullberg, 2008) and the microbiota is essential for the accumulation of both cell types (Ohnmacht et al., 2015; Lathrop et al., 2011; Atarashi et al., 2011; Yang et al., 2014; Nishio et al., 2015) in a process coined the “microbiota-T-cell axis” (Lee and Kim, 2017). From the GI tract’s luminal environment, immune-modulating signals are propagated through the gut epithelium to the antigen presenting dendritic cells and macrophages in the GALT. Here, naïve CD4$^+$ lymphocytes receive signals to differentiate into distinct T helper cell lineages, a process influenced by cytokines, master transcription factors and STAT proteins (Zhu and Paul, 2010). Th17 and Treg cells represent two CD4$^+$ T cell subsets with opposing principal functions, however, these cell types maintain a functional plasticity blurring their distinct phenotypes (Lochner et al., 2015). The inflammatory milieu determines how the RORγt^+ Foxp3$^+$ common CD4$^+$ precursors differentiate into either the proinflammatory Th17 cells or immunomodulatory Tregs. For example, Foxp3$^+$ Treg cells can be converted into IL-17 producing cells the presence of excessive IL-1β (Li et al., 2010).

This plasticity between the Th17 and Treg cell types could explain the minor discrepancies in the IL-17/IL-10 and *Rorγt/Foxp3* mRNA ratios in the current dataset. The ratio of IL-17/IL-10 in the serum of probiotic- and synbiotic-treated mice was significantly reduced; however, this was not observed in the PBMCs in the flow cytometry data. This could be a reflection of the general response of all the blood-derived immune cells against the specific response in the Treg and Th17 cell types. A similar argument could be made for the ratios of *Rorγt* to *Foxp3* mRNA levels where their ratio decreased in the control yet increased in the stressed group, which could be explained by alterations in the transitional Foxp3$^+$ Rorγt^+ CD4$^+$ cells that express both transcripts. Based on the flow cytometry data, it is clear that the

ratio of $IL10^+$ Tregs and $IL17^+$ $IL\text{-}23R^+$ Th17 activated cell populations are compromised due to chronic stress and preferentially upregulated by the synbiotic in the liver and ileum.

The gut microbiota and its metabolites guide the expansion of specific dendritic cell and macrophage subtypes generating a cytokine profile that drives differentiation of naive $CD4^+$ cells (Arpaia et al., 2013; Yadav et al., 2013). For example, SCFAs can stimulate tolerogenic $CD103^+$ dendritic cells (Hartog et al., 2015) to produce cytokines that induce $Foxp3^+$ Tregs (Jia et al., 2018) while polyphenols have also been linked to altered Treg and Th17 populations (Yahfoufi et al., 2018). Treg's can also be induced by specific microbiota populations including Clostridium clusters IV and XIVa (Atarashi et al., 2011), Lachnospiraceae and Ruminococcaceae (Han et al., 2018), and *L. reuteri* (Liu et al., 2014). In contrast, segmented filamentous bacteria produce soluble factors that drive differentiation of Th17 cells (Ivanov et al., 2009; Goto et al., 2014) whereas *Prevotella* spp. stimulate epithelial cells to produce cytokines that promote Th17 immune cell responses (Larsen, 2017). Since the synbiotic both produces metabolites and invokes specific changes in the gut microbiota, the impact on immune remodelling may be two-fold.

Investigating potential transcriptional regulators that are responsible for the synbiotic's overall impact on immune cell migratory patterns, the NanoString analysis revealed that the AHR is a predicted regulatory transcription factor in this regard. The AHR is ubiquitously expressed with concentrated levels in immune cells and acts as a mediator of dioxin toxicity, receptor for xenobiotics and metabolic products, including those derived from the gut microbiota (Grohmann and Puccetti, 2015). The AHR is critically involved in the immune response; although, its tissue- and time-dependent impact of LPS-mediated immune responses (Wu et al., 2011) demonstrates how the AHR is more involved in "fine-tuning" the adaptive immune response and maintenance of intestinal homeostasis (Korecka et al., 2016). In general, in mucosal immunity, AHR activation leads to decreased symptoms of intestinal inflammation (Takamura et al., 2010) primarily through increasing IL-22 production and regulating the development of innate lymphoid cells (ILCs) and intraepithelial lymphocytes (Gao et al., 2018; Zelante et al., 2014; Hubbard et al., 2015). This being said, it is important to emphasize the promiscuous nature of AHR signaling. There are many opposing studies both *in vitro* and *in vivo* regarding the downstream manifestation of AHR activity with the same ligands (Julliard et al., 2014; Sun et al., 2020). In general, the AHR is deemed protective, facilitating a positive feedback loop in response to its endogenous ligands to prevent the over-reactivity of an immune response with the induction of Tregs and other modulatory mechanisms, while exogenous pathogenic ligands can also act through the AHR to invoke proinflammatory, Th17-dominated responses. The current studies validate that the gut microbiota metabolites fall on the protective side of AHR signaling, stimulating Treg differentiation and promoting resilience to stress-induced inflammatory responses.

Arguably, the most important AHR ligands are the tryptophan metabolites including endogenous kynurenine and gut microbiota-derived indole-3-aldehyde, whose agonism increases the production of IL-22 (Zelante et al., 2013). Indeed, tryptophan metabolism shapes immune regulation through the AhR/IDO axis (Zelante et al., 2014). AHR agonism drives IDO, TDO, kynurenase and KMO expression, increasing kynurenine production in an autocrine loop of AHR activation (Vogel et al., 2008; Quintana et al., 2010). Importantly, the

AHR/IDO axis promotes Foxp3^{+} Treg cell production (Fallarino et al. (2006); Mezrich et al. (2010)) where in dendritic cell AHR knockouts *in vitro*, Treg expansion was suppressed with a disproportionate increase in Th17 cells (Nguyen et al., 2010). In a pulmonary fungal infection model, the IDO/AHR axis controlled the infection's severity by regulating the Treg/Th17 ratio (de Araújo et al., 2017). The impact of AHR reaches further than dendritic cells in the GI tract, as AHR activation in ILCs and gut intraepithelial lymphocytes shape the gut microbiota-host interaction in mucosal immunity (Gutiérrez-Vázquez and Quintana, 2018). As such, it has been suggested that AHR activation can alleviate the neuroinflammatory symptoms of multiple sclerosis (Rothhammer et al., 2016), the comorbidities between obesity and depression (Chaves Filho et al., 2018), and stroke (Chen et al., 2019). Importantly, in a model where exogenous kynurenine was injected into mice as a model of depressive-like behavior, the increase in neuroinflammation and chemotaxis of monocytes to the brain was shown to occur in a kynurenine- and AHR-dependent manner, mostly due to the upregulation of CCL2, which was dampened by an AHR ligand *in vitro* (Zang et al., 2018).

The influence of AHR on THP-1 cells' inflammatory phenotype was tested in an LPS-challenged gut epithelial coculture model. The AHR antagonist TMF reversed the synbiotic-induced decrease in IL-1β and kynurenine production to a level on par with LPS alone. This effect was only propagated in the metabolites 4HPAA, 4HPPA and CA and not the flavonoid metabolites 3′MeQ, 7′MeQ or Kamf, showing a significant metabolite-specific effect. In order to determine a causal mechanism of synbiotic-induced metabolites through the AHR, studies must be followed up by *in vivo* application of the bioactive metabolites in the chronic stress model. Polyphenols are known to have a promiscuous activity through the AHR (Zelante et al., 2014) and an early study using an *in vitro* bioassay for dioxins, marked AHR activation was exhibited by isoflavones such as daidzein, resveratrol, some flavanones such as naringenin, and flavones such as baicalein. On the other hand, some flavones, flavonols such as quercetin, and anthraquinones such as emodin inhibited AHR activity (Amakura et al., 2008). In other studies, quercetin, resveratrol and curcumin indirectly activated AHR activity (Mohammadi-Bardbori et al., 2012), 3-hydroxyflavone induced nuclear translocation and consequent AHR activation (Muku et al., 2018), while a battery of hydroxystilbenes and methoxystilbenes had general agonistic effects on the AHR receptor (Pastorková et al., 2017) confirming the diversity and complexity of gut-derived metabolites on the activity of the AHR receptor.

5. Conclusions

In conclusion, this study reveals a putative mechanism of gut-brain-axis signaling by which a synbiotic can attenuate the depressive- and anxiety-like behavioral deficits associated with chronic stress in male mice (Fig. 6). Although confirmation is required, synbiotic-specific metabolites may potentially act as a ligand to the AHR on antigen presenting cells or directly on the naïve CD4 + T cells, impacting their response to stress ultimately leading to reprogramming the proportions of the Treg and Th17 lymphocytes in the periphery. This resilience to inflammation in the periphery ultimately protects against neuroinflammation in the brain by altering the recruitment of immune cells and potentially protecting the integrity of the BBB. Further studies must be conducted to elucidate the impact of the peripheral

Treg/Th17 ratio on neuroinflammatory mediators; however, this study opens a new hypothesis and potential novel therapeutic strategy for treating stress-induced depression using synbiotics.

Supplementary Material

Refer to Web version on PubMed Central for supplementary material.

Acknowledgements

The authors would like to thank the staff at Mount Sinai's Center shared facility for Comparative Medicine and Surgery (CCMS) for animal and veterinary services. The authors would also like to thank the qPCR and Flow Cytometry cores of Mount Sinai, notably Nada Marjanovic for running the NanoString samples and Gina Viavattene and Chris Bare for the design and assisted running of the flow cytometry samples.

Funding Sources

This study was supported by Grant Number P50 AT008661-01 and U19 Grant Number AT010835 from the NCCIH and the ODS. Dr. Pasinetti holds a Senior VA Career Scientist Award. We acknowledge that the contents of this study do not represent the views of the NCCIH, the ODS, the NIH, the U.S. Department of Veterans Affairs, or the United States Government.

References

McEwen BS, 2004. Protection and damage from acute and chronic stress: allostasis and allostatic overload and relevance to the pathophysiology of psychiatric disorders. Ann N Y Acad Sci 1032, 1–7. [PubMed: 15677391]

Kobrosly RW, van Wijngaarden E, Seplaki CL, Cory-Slechta DA, Moynihan J, 2014. Depressive symptoms are associated with allostatic load among community-dwelling older adults. Physiol Behav 123, 223–230. [PubMed: 24432360]

Ullmann E, Perry SW, Licinio J, Wong ML, Dremencov E, Zavjalov EL, et al., 2019. From Allostatic Load to Allostatic State-An Endogenous Sympathetic Strategy to Deal With Chronic Anxiety and Stress? Front Behav Neurosci 13, 47. [PubMed: 30967764]

Wiley NC, Dinan TG, Ross RP, Stanton C, Clarke G, Cryan JF, 2017. The microbiota-gut-brain axis as a key regulator of neural function and the stress response: Implications for human and animal health. J Anim Sci 95 (7), 3225–3246. [PubMed: 28727115]

Westfall S, Pasinetti GM, 2019. The Gut Microbiota Links Dietary Polyphenols With Management of Psychiatric Mood Disorders. Front Neurosci 13, 1196. [PubMed: 31749681]

Bercik P, Denou E, Collins J, Jackson W, Lu J, Jury J, et al., 2011. The intestinal microbiota affect central levels of brain-derived neurotropic factor and behavior in mice. Gastroenterology. 141 (2), 599–609 e1–3. [PubMed: 21683077]

Zheng P, Zeng B, Zhou C, Liu M, Fang Z, Xu X, et al., 2016. Gut microbiome remodeling induces depressive-like behaviors through a pathway mediated by the host's metabolism. Mol Psychiatry. 21 (6), 786–796. [PubMed: 27067014]

Li N, Wang Q, Wang Y, Sun A, Lin Y, Jin Y, et al., 2019. Fecal microbiota transplantation from chronic unpredictable mild stress mice donors affects anxiety-like and depression-like behavior in recipient mice via the gut microbiota-inflammation-brain axis. Stress. 22 (5), 592–602. [PubMed: 31124390]

Langgartner D, Peterlik D, Foertsch S, Füchsl AM, Brokmann P, Flor PJ, et al., 2017. Individual differences in stress vulnerability: The role of gut pathobionts in stress-induced colitis. Brain Behav Immun 64, 23–32. [PubMed: 28012830]

Jiang H, Ling Z, Zhang Y, Mao H, Ma Z, Yin Y, et al., 2015. Altered fecal microbiota composition in patients with major depressive disorder. Brain Behav Immun 48, 186–194. [PubMed: 25882912]

Naseribafrouei A, Hestad K, Avershina E, Sekelja M, Linløkken A, Wilson R, et al., 2014. Correlation between the human fecal microbiota and depression. Neurogastroenterol Motil 26 (8), 1155–1162. [PubMed: 24888394]

Valles-Colomer M, Falony G, Darzi Y, Tigchelaar EF, Wang J, Tito RY, et al., 2019. The neuroactive potential of the human gut microbiota in quality of life and depression. Nat Microbiol 4 (4), 623–632. [PubMed: 30718848]

Galley JD, Yu Z, Kumar P, Dowd SE, Lyte M, Bailey MT, 2014. The structures of the colonic mucosa-associated and luminal microbial communities are distinct and differentially affected by a prolonged murine stressor. Gut Microbes 5 (6), 748–760. [PubMed: 25536463]

Ng QX, Peters C, Ho CYX, Lim DY, Yeo WS, 2018. A meta-analysis of the use of probiotics to alleviate depressive symptoms. J Affect Disord 228, 13–19. [PubMed: 29197739]

Haghighat N, Rajabi S, Mohammadshahi M, 2019. Effect of synbiotic and probiotic supplementation on serum brain-derived neurotrophic factor level, depression and anxiety symptoms in hemodialysis patients: a randomized, double-blinded, clinical trial. Nutr Neurosci 1–10.

Maqsood R, Stone TW, 2016. The Gut-Brain Axis, BDNF, NMDA and CNS Disorders. Neurochem Res 41 (11), 2819–2835. [PubMed: 27553784]

Desbonnet L, Clarke G, Traplin A, O'Sullivan O, Crispie F, Moloney RD, et al., 2015. Gut microbiota depletion from early adolescence in mice: Implications for brain and behaviour. Brain Behav Immun. 48, 165–173. [PubMed: 25866195]

Mayer EA, Tillisch K, Gupta A, 2015. Gut/brain axis and the microbiota. J Clin Invest. 125 (3), 926–938. [PubMed: 25689247]

Bellono NW Bayrer JR Leitch DB Castro J Zhang C O'Donnell TA et al. Enterochromaffin Cells Are Gut Chemosensors that Couple to Sensory Neural Pathways Cell. 170 1 2017 185 98.e16. [PubMed: 28648659]

Dehhaghi M Kazemi Shariat Panahi H GJ. G Microorganisms Tryptophan Metabolism, and Kynurenine Pathway: A Complex Interconnected Loop Influencing Human Health Status Int J Tryptophan Res 2019;12:1178646919852996. [PubMed: 31258331]

Gao J, Xu K, Liu H, Liu G, Bai M, Peng C, et al., 2018a. Impact of the Gut Microbiota on Intestinal Immunity Mediated by Tryptophan Metabolism. Front Cell Infect Microbiol 8, 13. [PubMed: 29468141]

Kim YK, Jeon SW, 2018. Neuroinflammation and the Immune-Kynurenine Pathway in Anxiety Disorders. Curr Neuropharmacol 16 (5), 574–582. [PubMed: 28901278]

Zang X, Zheng X, Hou Y, Hu M, Wang H, Bao X, et al., 2018. Regulation of proinflammatory monocyte activation by the kynurenine-AhR axis underlies immunometabolic control of depressive behavior in mice. Faseb j. 32 (4), 1944–1956. [PubMed: 29183965]

Thaiss CA, Zmora N, Levy M, Elinav E, 2016. The microbiome and innate immunity. Nature. 535 (7610), 65–74. [PubMed: 27383981]

Britanova L, Diefenbach A, 2017. Interplay of innate lymphoid cells and the microbiota. Immunol Rev 279 (1), 36–51. [PubMed: 28856740]

Blander JM, Longman RS, Iliev ID, Sonnenberg GF, Artis D, 2017. Regulation of inflammation by microbiota interactions with the host. Nat Immunol 18 (8), 851–860. [PubMed: 28722709]

Koboziev I, Karlsson F, Grisham MB, 2010. Gut-associated lymphoid tissue, T cell trafficking, and chronic intestinal inflammation. Ann N Y Acad Sci 1207 Suppl 1 (Suppl 1), E86–E93. [PubMed: 20961311]

Arpaia N, Campbell C, Fan X, Dikiy S, van der Veeken J, deRoos P, et al., 2013. Metabolites produced by commensal bacteria promote peripheral regulatory T-cell generation. Nature. 504 (7480), 451–455. [PubMed: 24226773]

Luo A, Leach ST, Barres R, Hesson LB, Grimm MC, Simar D, 2017. The Microbiota and Epigenetic Regulation of T Helper 17/Regulatory T Cells. In Search of a Balanced Immune System. Front Immunol 8, 417.

Cui H, Cai Y, Wang L, Jia B, Li J, Zhao S, et al., 2018. Berberine Regulates Treg/Th17 Balance to Treat Ulcerative Colitis Through Modulating the Gut Microbiota in the Colon. Front Pharmacol. 9, 571. [PubMed: 29904348]

Britton GJ Contijoch EJ Mogno I Vennaro OH Llewellyn SR Ng R et al. Microbiotas from Humans with Inflammatory Bowel Disease Alter the Balance of Gut Th17 and RORγt(+) Regulatory T Cells and Exacerbate Colitis in Mice Immunity. 50 1 2019 212 24.e4. [PubMed: 30650377]

Hong M, Zheng J, Ding ZY, Chen JH, Yu L, Niu Y, et al., 2013. Imbalance between Th17 and Treg cells may play an important role in the development of chronic unpredictable mild stress-induced depression in mice. Neuroimmunomodulation. 20 (1), 39–50. [PubMed: 23172104]

Jurado-Manzano BB, Zavala-Reyes D, Turrubiartes-Martínez EA, Portales-Pérez DP, González-Amaro R, Layseca-Espinosa E, 2017. FICZ generates human tDCs that induce CD4(+) CD25(high) Foxp3(+) Treg-like cell differentiation. Immunol Lett 190, 84–92. [PubMed: 28765071]

Shi C, Zhang H, Wang X, Jin B, Jia Q, Li Y, et al., 2020. Cinnamtannin D1 attenuates autoimmune arthritis by regulating the balance of Th17 and treg cells through inhibition of aryl hydrocarbon receptor expression. Pharmacol Res 151, 104513. [PubMed: 31706010]

Tong B, Yuan X, Dou Y, Wu X, Chou G, Wang Z, et al., 2016. Norisoboldine, an isoquinoline alkaloid, acts as an aryl hydrocarbon receptor ligand to induce intestinal Treg cells and thereby attenuate arthritis. Int J Biochem Cell Biol 75, 63–73. [PubMed: 27032495]

Zelante T, Iannitti RG, Cunha C, De Luca A, Giovannini G, Pieraccini G, et al., 2013. Tryptophan catabolites from microbiota engage aryl hydrocarbon receptor and balance mucosal reactivity via interleukin-22. Immunity. 39 (2), 372–385. [PubMed: 23973224]

Veldhoen M, Hirota K, Westendorf AM, Buer J, Dumoutier L, Renauld JC, et al., 2008. The aryl hydrocarbon receptor links TH17-cell-mediated autoimmunity to environmental toxins. Nature. 453 (7191), 106–109. [PubMed: 18362914]

Quintana FJ, Basso AS, Iglesias AH, Korn T, Farez MF, Bettelli E, et al., 2008. Control of T(reg) and T(H)17 cell differentiation by the aryl hydrocarbon receptor. Nature. 453 (7191), 65–71. [PubMed: 18362915]

Frolinger T, Sims S, Smith C, Wang J, Cheng H, Faith J, et al., 2019. The gut microbiota composition affects dietary polyphenols-mediated cognitive resilience in mice by modulating the bioavailability of phenolic acids. Sci Rep 9 (1), 3546. [PubMed: 30837576]

Frolinger T, Herman F, Sharma A, Sims S, Wang J, Pasinetti GM, 2018. Epigenetic modifications by polyphenolic compounds alter gene expression in the hippocampus. Biol Open. 7 (10).

Wang J, Hodes GE, Zhang H, Zhang S, Zhao W, Golden SA, et al., 2018. Epigenetic modulation of inflammation and synaptic plasticity promotes resilience against stress in mice. Nat Commun 9 (1), 477. [PubMed: 29396460]

van den Nieuwboer M, van Hemert S, Claassen E, de Vos WM, 2016. Lactobacillus plantarum WCFS1 and its host interaction: a dozen years after the genome. Microb Biotechnol 9 (4), 452–465. [PubMed: 27231133]

Pinto-Sanchez MI Hall GB Ghajar K Nardelli A Bolino C Lau JT et al. Probiotic Bifidobacterium longum NCC3001 Reduces Depression Scores and Alters Brain Activity: A Pilot Study in Patients With Irritable Bowel Syndrome Gastroenterology. 153 2 2017 448 59.e8. [PubMed: 28483500]

Hodes GE, Pfau ML, Purushothaman I, Ahn HF, Golden SA, Christoffel DJ, et al., 2015. Sex Differences in Nucleus Accumbens Transcriptome Profiles Associated with Susceptibility versus Resilience to Subchronic Variable Stress. J Neurosci 35 (50), 16362–16376. [PubMed: 26674863]

Frolinger T, Smith C, Cobo CF, Sims S, Brathwaite J, de Boer S, et al., 2018. Dietary polyphenols promote resilience against sleep deprivation-induced cognitive impairment by activating protein translation. Faseb j. 32 (10), 5390–5404. [PubMed: 29702026]

Seibenhener ML, Wooten MC, 2015. Use of the Open Field Maze to measure locomotor and anxiety-like behavior in mice. J Vis Exp 96, e52434.

Can A, Dao DT, Arad M, Terrillion CE, Piantadosi SC, Gould TD, 2012. The mouse forced swim test. J Vis Exp 59, e3638.

Ho L, Zhao D, Ono K, Ruan K, Mogno I, Tsuji M, et al., 2019. Heterogeneity in gut microbiota drive polyphenol metabolism that influences α-synuclein misfolding and toxicity. The Journal of Nutritional Biochemistry. 64, 170–181. [PubMed: 30530257]

Livak KJ, Schmittgen TD, 2001. Analysis of relative gene expression data using real-time quantitative PCR and the 2(-Delta Delta C(T)) Method. Methods. 25 (4), 402–408. [PubMed: 11846609]

Ottaviani JI, Fong R, Kimball J, Ensunsa JL, Britten A, Lucarelli D, et al., 2018. Evaluation at scale of microbiome-derived metabolites as biomarker of flavan-3-ol intake in epidemiological studies. Scientific Reports. 8 (1), 9859. [PubMed: 29959422]

Camilleri M, 2009. Serotonin in the gastrointestinal tract. Curr Opin Endocrinol Diabetes Obes 16 (1), 53–59. [PubMed: 19115522]

Chavan SS, Pavlov VA, Tracey KJ, 2017. Mechanisms and Therapeutic Relevance of Neuro-immune Communication. Immunity. 46 (6), 927–942. [PubMed: 28636960]

Han B, Yu L, Geng Y, Shen L, Wang H, Wang Y, et al., 2016. Chronic Stress Aggravates Cognitive Impairment and Suppresses Insulin Associated Signaling Pathway in APP/PS1 Mice. J Alzheimers Dis 53 (4), 1539–1552. [PubMed: 27392857]

Kawasaki T, Kawai T, 2014. Toll-like receptor signaling pathways. Front Immunol 5, 461. [PubMed: 25309543]

Lamas B, Natividad JM, Sokol H, 2018. Aryl hydrocarbon receptor and intestinal immunity. Mucosal Immunol 11 (4), 1024–1038. [PubMed: 29626198]

Gutiérrez-Vázquez C, Quintana FJ, 2018. Regulation of the Immune Response by the Aryl Hydrocarbon Receptor. Immunity. 48 (1), 19–33. [PubMed: 29343438]

Diller ML, Kudchadkar RR, Delman KA, Lawson DH, Ford ML, 2016. Balancing Inflammation: The Link between Th17 and Regulatory T Cells. Mediators Inflamm 2016, 6309219. [PubMed: 27413254]

Nguyen LP, Bradfield CA, 2008. The search for endogenous activators of the aryl hydrocarbon receptor. Chem Res Toxicol 21 (1), 102–116. [PubMed: 18076143]

Burokas A, Arboleya S, Moloney RD, Peterson VL, Murphy K, Clarke G, et al., 2017. Targeting the Microbiota-Gut-Brain Axis: Prebiotics Have Anxiolytic and Antidepressant-like Effects and Reverse the Impact of Chronic Stress in Mice. Biol Psychiatry. 82 (7), 472–487. [PubMed: 28242013]

Liang S, Wang T, Hu X, Luo J, Li W, Wu X, et al., 2015. Administration of Lactobacillus helveticus NS8 improves behavioral, cognitive, and biochemical aberrations caused by chronic restraint stress. Neuroscience. 310, 561–577. [PubMed: 26408987]

Strandwitz P, 2018. Neurotransmitter modulation by the gut microbiota. Brain Res 1693 (Pt B), 128–133. [PubMed: 29903615]

Clark A, Mach N, 2016. Exercise-induced stress behavior, gut-microbiota-brain axis and diet: a systematic review for athletes. J Int Soc Sports Nutr 13, 43. [PubMed: 27924137]

Petra AI, Panagiotidou S, Hatziagelaki E, Stewart JM, Conti P, Theoharides TC, 2015. Gut-Microbiota-Brain Axis and Its Effect on Neuropsychiatric Disorders With Suspected Immune Dysregulation. Clin Ther 37 (5), 984–995. [PubMed: 26046241]

Mahar I, Bambico FR, Mechawar N, Nobrega JN, 2014. Stress, serotonin, and hippocampal neurogenesis in relation to depression and antidepressant effects. Neurosci Biobehav Rev 38, 173–192. [PubMed: 24300695]

Vaghef-Mehrabany E, Maleki V, Behrooz M, Ranjbar F, Ebrahimi-Mameghani M, 2019. Can psychobiotics “mood” ify gut? An update systematic review of randomized controlled trials in healthy and clinical subjects, on anti-depressant effects of probiotics, prebiotics, and synbiotics. Clin Nutr

Gurry T, 2017. Synbiotic approaches to human health and well-being. Microb Biotechnol 10 (5), 1070–1073. [PubMed: 28771949]

Bourin M, Fiocco AJ, Clenet F, 2001. How valuable are animal models in defining antidepressant activity? Hum Psychopharmacol 16 (1), 9–21. [PubMed: 12404593]

O’Mahony SM, Clarke G, Borre YE, Dinan TG, Cryan JF, 2015. Serotonin, tryptophan metabolism and the brain-gut-microbiome axis. Behav Brain Res 277, 32–48. [PubMed: 25078296]

Clarke G, McKernan DP, Gaszner G, Quigley EM, Cryan JF, Dinan TG, 2012. A Distinct Profile of Tryptophan Metabolism along the Kynurenine Pathway Downstream of Toll-Like Receptor Activation in Irritable Bowel Syndrome. Front Pharmacol 3, 90. [PubMed: 22661947]

Martin-Gallausiaux C, Larraufie P, Jarry A, Béguet-Crespel F, Marinelli L, Ledue F, et al., 2018. Butyrate Produced by Commensal Bacteria Down-Regulates Indolamine 2,3-Dioxygenase 1

(IDO-1) Expression via a Dual Mechanism in Human Intestinal Epithelial Cells. Front Immunol 9, 2838. [PubMed: 30619249]

Waclawiková B, El Aidy S, 2018. Role of Microbiota and Tryptophan Metabolites in the Remote Effect of Intestinal Inflammation on Brain and Depression. Pharmaceuticals (Basel) 11 (3).

Schulz S, Landi A, Garg R, Wilson JA, 2015. van Drunen Littel-van den Hurk S. Indolamine 2,3-dioxygenase expression by monocytes and dendritic cell populations in hepatitis C patients. Clin Exp Immunol 180 (3), 484–498. [PubMed: 25605587]

Stone TW, Stoy N, Darlington LG, 2013. An expanding range of targets for kynurenine metabolites of tryptophan. Trends Pharmacol Sci 34 (2), 136–143. [PubMed: 23123095]

Steiner J, Walter M, Gos T, Guillemin GJ, Bernstein HG, Sarnyai Z, et al., 2011. Severe depression is associated with increased microglial quinolinic acid in subregions of the anterior cingulate gyrus: evidence for an immune-modulated glutamatergic neurotransmission? J Neuroinflammation 8, 94. [PubMed: 21831269]

Savitz J, 2017. Role of Kynurenine Metabolism Pathway Activation in Major Depressive Disorders. Curr Top Behav Neurosci 31, 249–267. [PubMed: 27221627]

Brundin L, Sellgren CM, Lim CK, Grit J, Pålsson E, Landén M, et al., 2016. An enzyme in the kynurenine pathway that governs vulnerability to suicidal behavior by regulating excitotoxicity and neuroinflammation. Transl Psychiatry. 6 (8), e865. [PubMed: 27483383]

Jones SP, Franco NF, Varney B, Sundaram G, Brown DA, de Bie J, et al., 2015. Expression of the Kynurenine Pathway in Human Peripheral Blood Mononuclear Cells: Implications for Inflammatory and Neurodegenerative Disease. PLoS One. 10 (6), e0131389. [PubMed: 26114426]

Zhang S, Sakuma M, Deora GS, Levy CW, Klausing A, Breda C, et al., 2019. A brain-permeable inhibitor of the neurodegenerative disease target kynurenine 3-monooxygenase prevents accumulation of neurotoxic metabolites. Commun Biol 2, 271. [PubMed: 31372510]

Kim YK, Won E, 2017. The influence of stress on neuroinflammation and alterations in brain structure and function in major depressive disorder. Behav Brain Res 329, 6–11. [PubMed: 28442354]

Dinkel K, MacPherson A, Sapolsky RM, 2003. Novel glucocorticoid effects on acute inflammation in the CNS. J Neurochem 84 (4), 705–716. [PubMed: 12562515]

Munhoz CD, Sorrells SF, Caso JR, Scavone C, Sapolsky RM, 2010. Glucocorticoids exacerbate lipopolysaccharide-induced signaling in the frontal cortex and hippocampus in a dose-dependent manner. J Neurosci 30 (41), 13690–13698. [PubMed: 20943909]

Koo JW, Russo SJ, Ferguson D, Nestler EJ, Duman RS, 2010. Nuclear factor-kappaB is a critical mediator of stress-impaired neurogenesis and depressive behavior. Proc Natl Acad Sci U S A. 107 (6), 2669–2674. [PubMed: 20133768]

Dowlati Y, Herrmann N, Swardfager W, Liu H, Sham L, Reim EK, et al., 2010. A meta-analysis of cytokines in major depression. Biol Psychiatry. 67 (5), 446–457. [PubMed: 20015486]

Howren MB, Lamkin DM, Suls J, 2009. Associations of depression with C-reactive protein, IL-1, and IL-6: a meta-analysis. Psychosom Med 71 (2), 171–186. [PubMed: 19188531]

Torres-Platas SG, Cruceanu C, Chen GG, Turecki G, Mechawar N, 2014. Evidence for increased microglial priming and macrophage recruitment in the dorsal anterior cingulate white matter of depressed suicides. Brain Behav Immun 42, 50–59. [PubMed: 24858659]

D'Mello C, Le T, Swain MG, 2009. Cerebral microglia recruit monocytes into the brain in response to tumor necrosis factoralpha signaling during peripheral organ inflammation. J Neurosci 29 (7), 2089–2102. [PubMed: 19228962]

Walker AK, Kavelaars A, Heijnen CJ, Dantzer R, 2014. Neuroinflammation and comorbidity of pain and depression. Pharmacol Rev 66 (1), 80–101. [PubMed: 24335193]

Wohleb ES, McKim DB, Shea DT, Powell ND, Tarr AJ, Sheridan JF, et al., 2014. Re-establishment of anxiety in stress-sensitized mice is caused by monocyte trafficking from the spleen to the brain. Biol Psychiatry 75 (12), 970–981. [PubMed: 24439304]

Seo JS, Wei J, Qin L, Kim Y, Yan Z, Greengard P, 2017. Cellular and molecular basis for stress-induced depression. Mol Psychiatry 22 (10), 1440–1447. [PubMed: 27457815]

Belleau EL, Treadway MT, Pizzagalli DA, 2019. The Impact of Stress and Major Depressive Disorder on Hippocampal and Medial Prefrontal Cortex Morphology. Biol Psychiatry 85 (6), 443–453. [PubMed: 30470559]

Tomita M, Khan RL, Blehm BH, Santoro TJ, 2004. The potential pathogenetic link between peripheral immune activation and the central innate immune response in neuropsychiatric systemic lupus erythematosus. Med Hypotheses. 62 (3), 325–335. [PubMed: 14975498]

Fuzzati-Armentero MT, Cerri S, Blandini F, 2019. Peripheral-Central Neuroimmune Crosstalk in Parkinson's Disease: What Do Patients and Animal Models Tell Us? Front Neurol 10, 232. [PubMed: 30941089]

Park J, Baik SH, Mook-Jung I, Irimia D, Cho H, 2019. Mimicry of Central-Peripheral Immunity in Alzheimer's Disease and Discovery of Neurodegenerative Roles in Neutrophil. Front Immunol 10, 2231. [PubMed: 31611872]

Dionisio-Santos DA, Olschowka JA, O'Banion MK, 2019. Exploiting microglial and peripheral immune cell crosstalk to treat Alzheimer's disease. J Neuroinflammation. 16 (1), 74. [PubMed: 30953557]

Kempuraj D, Thangavel R, Selvakumar GP, Zaheer S, Ahmed ME, Raikwar SP, et al., 2017. Brain and Peripheral Atypical Inflammatory Mediators Potentiate Neuroinflammation and Neurodegeneration. Front Cell Neurosci 11, 216. [PubMed: 28790893]

Wang Y, Xu J, Liu Y, Li Z, Li X, 2018. TLR4-NF-κB Signal Involved in Depressive-Like Behaviors and Cytokine Expression of Frontal Cortex and Hippocampus in Stressed C57BL/6 and ob/ob Mice. Neural Plast 2018, 7254016. [PubMed: 29765402]

Herman FJ, Pasinetti GM, 2018. Principles of inflammasome priming and inhibition: Implications for psychiatric disorders. Brain Behav Immun 73, 66–84. [PubMed: 29902514]

Zhang Y, Liu L, Liu YZ, Shen XL, Wu TY, Zhang T, et al., 2015. NLRP3 Inflammasome Mediates Chronic Mild Stress-Induced Depression in Mice via Neuroinflammation. Int J Neuropsychopharmacol 18 (8).

Mao L, Kitani A, Strober W, Fuss IJ, 2018. The Role of NLRP3 and IL-1β in the Pathogenesis of Inflammatory Bowel Disease. Front Immunol 9, 2566. [PubMed: 30455704]

Mak'Anyengo R, Duewell P, Reichl C, Hörth C, Lehr HA, Fischer S, et al., 2018. Nlrp3-dependent IL-1β inhibits CD103+ dendritic cell differentiation in the gut. JCI. Insight 3 (5).

Filardy AA, He J, Bennink J, Yewdell J, Kelsall BL, 2016. Posttranscriptional control of NLRP3 inflammasome activation in colonic macrophages. Mucosal Immunol 9 (4), 850–858. [PubMed: 26627461]

Wohleb ES, McKim DB, Sheridan JF, Godbout JP, 2014. Monocyte trafficking to the brain with stress and inflammation: a novel axis of immune-to-brain communication that influences mood and behavior. Front Neurosci 8, 447. [PubMed: 25653581]

Wohleb ES, Powell ND, Godbout JP, Sheridan JF, 2013. Stress-induced recruitment of bone marrow-derived monocytes to the brain promotes anxiety-like behavior. J Neurosci 33 (34), 13820–13833. [PubMed: 23966702]

Dhabhar FS, Malarkey WB, Neri E, McEwen BS, 2012. Stress-induced redistribution of immune cells–from barracks to boulevards to battlefields: a tale of three hormones–Curt Richter Award winner. Psychoneuroendocrinology. 37 (9), 1345–1368. [PubMed: 22727761]

Gao X, Cao Q, Cheng Y, Zhao D, Wang Z, Yang H, et al., 2018b. Chronic stress promotes colitis by disturbing the gut microbiota and triggering immune system response. Proc Natl Acad Sci U S A. 115 (13), E2960–E2969. [PubMed: 29531080]

Yan H, Baldridge MT, King KY, 2018. Hematopoiesis and the bacterial microbiome. Blood. 132 (6), 559–564. [PubMed: 29853538]

Zapolska-Downar D, Siennicka A, Kaczmarczyk M, Kołodziej B, Naruszewicz M, 2004. Butyrate inhibits cytokine-induced VCAM-1 and ICAM-1 expression in cultured endothelial cells: the role of NF-kappaB and PPARalpha. J Nutr Biochem 15 (4), 220–228. [PubMed: 15068815]

Maa MC, Chang MY, Hsieh MY, Chen YJ, Yang CJ, Chen ZC, et al., 2010. Butyrate reduced lipopolysaccharide-mediated macrophage migration by suppression of Src enhancement and focal adhesion kinase activity. J Nutr Biochem 21 (12), 1186–1192. [PubMed: 20149623]

Gonçalves P, Araújo JR, Di Santo JP, 2018. A Cross-Talk Between Microbiota-Derived Short-Chain Fatty Acids and the Host Mucosal Immune System Regulates Intestinal Homeostasis and Inflammatory Bowel Disease. Inflamm Bowel Dis 24 (3), 558–572. [PubMed: 29462379]

Cicha I, Regler M, Urschel K, Goppelt-Struebe M, Daniel WG, Garlichs CD, 2011. Resveratrol inhibits monocytic cell chemotaxis to MCP-1 and prevents spontaneous endothelial cell migration through Rho kinase-dependent mechanism. J Atheroscler Thromb 18 (12), 1031–1042. [PubMed: 21878744]

Bao L, Zhang Z, Dai X, Ding Y, Jiang Y, Li Y, et al., 2015. Effects of grape seed proanthocyanidin extract on renal injury in type 2 diabetic rats. Mol Med Rep 11 (1), 645–652. [PubMed: 25351255]

Lee CC, Kim JH, Kim JS, Oh YS, Han SM, Park JHY, et al., 2017. 5-(3',4'-Dihydroxyphenyl-γ-valerolactone), a Major Microbial Metabolite of Proanthocyanidin, Attenuates THP-1 Monocyte-Endothelial Adhesion. Int J Mol Sci 18 (7).

Koga T, Meydani M, 2001. Effect of plasma metabolites of (+)-catechin and quercetin on monocyte adhesion to human aortic endothelial cells. Am J Clin Nutr 73 (5), 941–948. [PubMed: 11333849]

Maloy KJ, Kullberg MC, 2008. IL-23 and Th17 cytokines in intestinal homeostasis. Mucosal Immunol 1 (5), 339–349. [PubMed: 19079198]

Ohnmacht C, Park JH, Cording S, Wing JB, Atarashi K, Obata Y, et al., 2015. MUCOSAL IMMUNOLOGY. The microbiota regulates type 2 immunity through RORγt$^+$ T cells. Science. 349 (6251), 989–993. [PubMed: 26160380]

Lathrop SK, Bloom SM, Rao SM, Nutsch K, Lio CW, Santacruz N, et al., 2011. Peripheral education of the immune system by colonic commensal microbiota. Nature. 478 (7368), 250–254. [PubMed: 21937990]

Atarashi K, Tanoue T, Shima T, Imaoka A, Kuwahara T, Momose Y, et al., 2011. Induction of colonic regulatory T cells by indigenous Clostridium species. Science. 331 (6015), 337–341. [PubMed: 21205640]

Yang Y, Torchinsky MB, Gobert M, Xiong H, Xu M, Linehan JL, et al., 2014. Focused specificity of intestinal TH17 cells towards commensal bacterial antigens. Nature. 510 (7503), 152–156. [PubMed: 24739972]

Nishio J, Baba M, Atarashi K, Tanoue T, Negishi H, Yanai H, et al., 2015. Requirement of full TCR repertoire for regulatory T cells to maintain intestinal homeostasis. Proc Natl Acad Sci U S A. 112 (41), 12770–12775. [PubMed: 26420876]

Lee N, Kim WU, 2017. Microbiota in T-cell homeostasis and inflammatory diseases. Exp Mol Med 49 (5), e340. [PubMed: 28546563]

Zhu J, Paul WE, 2010. Heterogeneity and plasticity of T helper cells. Cell Res 20 (1), 4–12. [PubMed: 20010916]

Lochner M, Wang Z, Sparwasser T, 2015. The Special Relationship in the Development and Function of T Helper 17 and Regulatory T Cells. Prog Mol Biol Transl Sci 136, 99–129. [PubMed: 26615094]

Li L, Kim J, Boussiotis VA, 2010. IL-1β-mediated signals preferentially drive conversion of regulatory T cells but not conventional T cells into IL-17-producing cells. J Immunol 185 (7), 4148–4153. [PubMed: 20817874]

Yadav M, Stephan S, Bluestone JA, 2013. Peripherally induced tregs - role in immune homeostasis and autoimmunity. Front Immunol 4, 232. [PubMed: 23966994]

Hartog A, Belle FN, Bastiaans J, de Graaff P, Garssen J, Harthoorn LF, et al., 2015. A potential role for regulatory T-cells in the amelioration of DSS induced colitis by dietary non-digestible polysaccharides. J Nutr Biochem 26 (3), 227–233. [PubMed: 25498760]

Jia L, Lu J, Zhou Y, Tao Y, Xu H, Zheng W, et al., 2018. Tolerogenic dendritic cells induced the enrichment of CD4(+)Foxp3(+) regulatory T cells via TGF-β in mesenteric lymph nodes of murine LPS-induced tolerance model. Clin Immunol 197, 118–129. [PubMed: 30248398]

Yahfoufi N, Alsadi N, Jambi M, Matar C, 2018. The Immunomodulatory and Anti-Inflammatory Role of Polyphenols. Nutrients. 10 (11).

Han L, Jin H, Zhou L, Zhang X, Fan Z, Dai M, et al., 2018. Intestinal Microbiota at Engraftment Influence Acute Graft-Versus-Host Disease via the Treg/Th17 Balance in Allo-HSCT Recipients. Front Immunol 9, 669. [PubMed: 29740427]

Liu Y, Tran DQ, Fatheree NY, Marc RJ, 2014. Lactobacillus reuteri DSM 17938 differentially modulates effector memory T cells and Foxp3+ regulatory T cells in a mouse model of necrotizing enterocolitis. Am J Physiol Gastrointest Liver Physiol 307 (2), G177–G186. [PubMed: 24852566]

Ivanov II, Atarashi K, Manel N, Brodie EL, Shima T, Karaoz U, et al., 2009. Induction of intestinal Th17 cells by segmented filamentous bacteria. Cell. 139 (3), 485–498. [PubMed: 19836068]

Goto Y, Panea C, Nakato G, Cebula A, Lee C, Diez MG, et al., 2014. Segmented filamentous bacteria antigens presented by intestinal dendritic cells drive mucosal Th17 cell differentiation. Immunity. 40 (4), 594–607. [PubMed: 24684957]

Larsen JM, 2017. The immune response to Prevotella bacteria in chronic inflammatory disease. Immunology. 151 (4), 363–374. [PubMed: 28542929]

Grohmann U, Puccetti P, 2015. The Coevolution of IDO1 and AhR in the Emergence of Regulatory T-Cells in Mammals. Front Immunol 6, 58. [PubMed: 25729384]

Wu D, Li W, Lok P, Matsumura F, Vogel CF, 2011. AhR deficiency impairs expression of LPS-induced inflammatory genes in mice. Biochem Biophys Res Commun 410 (2), 358–363. [PubMed: 21683686]

Korecka A, Dona A, Lahiri S, Tett AJ, Al-Asmakh M, Braniste V, et al., 2016. Bidirectional communication between the Aryl hydrocarbon Receptor (AhR) and the microbiome tunes host metabolism. NPJ Biofilms Microbiomes 2, 16014. [PubMed: 28721249]

Takamura T, Harama D, Matsuoka S, Shimokawa N, Nakamura Y, Okumura K, et al., 2010. Activation of the aryl hydrocarbon receptor pathway may ameliorate dextran sodium sulfate-induced colitis in mice. Immunol Cell Biol 88 (6), 685–689. [PubMed: 20231854]

Zelante T, Iannitti RG, Fallarino F, Gargaro M, De Luca A, Moretti S, et al., 2014. Tryptophan Feeding of the IDO1-AhR Axis in Host-Microbial Symbiosis. Front Immunol 5, 640. [PubMed: 25566253]

Hubbard TD, Murray IA, Bisson WH, Lahoti TS, Gowda K, Amin SG, et al., 2015. Adaptation of the human aryl hydrocarbon receptor to sense microbiota-derived indoles. Sci Rep 5, 12689. [PubMed: 26235394]

Julliard W, Fechner JH, Mezrich JD, 2014. The aryl hydrocarbon receptor meets immunology: friend or foe? A little of both. Front Immunol 5, 458. [PubMed: 25324842]

Sun M, Ma N, He T, Johnston LJ, Ma X, 2020. Tryptophan (Trp) modulates gut homeostasis via aryl hydrocarbon receptor (AhR). Crit Rev Food Sci Nutr 60 (10), 1760–1768. [PubMed: 30924357]

Vogel CF, Goth SR, Dong B, Pessah IN, Matsumura F, 2008. Aryl hydrocarbon receptor signaling mediates expression of indoleamine 2,3-dioxygenase. Biochem Biophys Res Commun 375 (3), 331–335. [PubMed: 18694728]

Quintana FJ, Murugaiyan G, Farez MF, Mitsdoerffer M, Tukpah AM, Burns EJ, et al., 2010. An endogenous aryl hydrocarbon receptor ligand acts on dendritic cells and T cells to suppress experimental autoimmune encephalomyelitis. Proc Natl Acad Sci U S A. 107 (48), 20768–20773. [PubMed: 21068375]

Fallarino F, Grohmann U, You S, McGrath BC, Cavener DR, Vacca C, et al., 2006. The combined effects of tryptophan starvation and tryptophan catabolites down-regulate T cell receptor zeta-chain and induce a regulatory phenotype in naive T cells. J Immunol 176 (11), 6752–6761. [PubMed: 16709834]

Mezrich JD, Fechner JH, Zhang X, Johnson BP, Burlingham WJ, Bradfield CA, 2010. An interaction between kynurenine and the aryl hydrocarbon receptor can generate regulatory T cells. J Immunol 185 (6), 3190–3198. [PubMed: 20720200]

Nguyen NT, Kimura A, Nakahama T, Chinen I, Masuda K, Nohara K, et al., 2010. Aryl hydrocarbon receptor negatively regulates dendritic cell immunogenicity via a kynurenine-dependent mechanism. Proc Natl Acad Sci U S A. 107 (46), 19961–19966. [PubMed: 21041655]

de Araújo EF, Feriotti C, Galdino NAL, Preite NW, Calich VLG, Loures FV, 2017. The IDO-AhR Axis Controls Th17/Treg Immunity in a Pulmonary Model of Fungal Infection. Front Immunol 8, 880. [PubMed: 28791025]

Rothhammer V, Mascanfroni ID, Bunse L, Takenaka MC, Kenison JE, Mayo L, et al., 2016. Type I interferons and microbial metabolites of tryptophan modulate astrocyte activity and central

nervous system inflammation via the aryl hydrocarbon receptor. Nat Med 22 (6), 586–597. [PubMed: 27158906]

Chaves Filho AJM, Lima CNC, Vasconcelos SMM, de Lucena DF, Maes M, Macedo D, 2018. IDO chronic immune activation and tryptophan metabolic pathway: A potential pathophysiological link between depression and obesity. Prog Neuropsychopharmacol Biol Psychiatry. 80 (Pt C), 234–249. [PubMed: 28595944]

Chen WC, Chang LH, Huang SS, Huang YJ, Chih CL, Kuo HC, et al., 2019. Aryl hydrocarbon receptor modulates stroke-induced astrogliosis and neurogenesis in the adult mouse brain. J Neuroinflammation. 16 (1), 187. [PubMed: 31606043]

Amakura Y, Tsutsumi T, Sasaki K, Nakamura M, Yoshida T, Maitani T, 2008. Influence of food polyphenols on aryl hydrocarbon receptor-signaling pathway estimated by in vitro bioassay. Phytochemistry. 69 (18), 3117–3130. [PubMed: 17869316]

Mohammadi-Bardbori A, Bengtsson J, Rannug U, Rannug A, Wincent E, 2012. Quercetin, resveratrol, and curcumin are indirect activators of the aryl hydrocarbon receptor (AHR). Chem Res Toxicol 25 (9), 1878–1884. [PubMed: 22867086]

Muku GE, Murray IA, Espín JC, Perdew GH, 2018. Urolithin A Is a Dietary Microbiota-Derived Human Aryl Hydrocarbon Receptor Antagonist. Metabolites. 8 (4).

Pastorková B, Vrzalová A, Bachleda P, Dvořák Z, 2017. Hydroxystilbenes and methoxystilbenes activate human aryl hydrocarbon receptor and induce CYP1A genes in human hepatoma cells and human hepatocytes. Food Chem Toxicol 103, 122–132. [PubMed: 28279696]

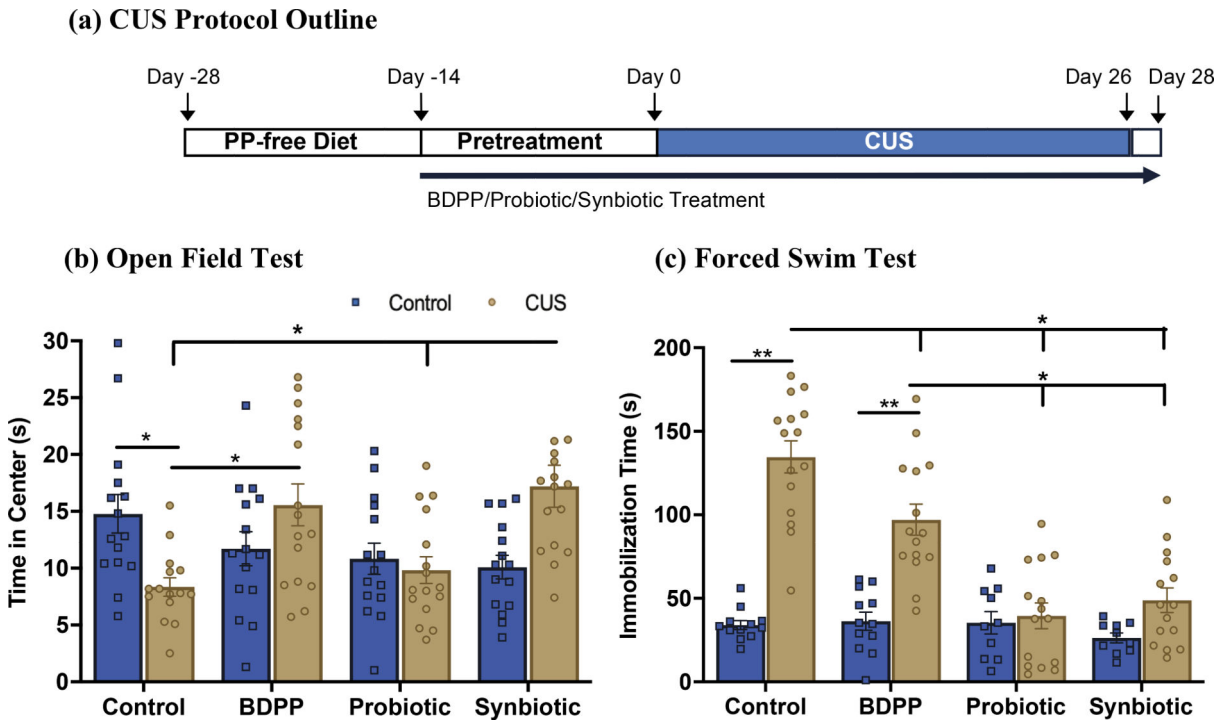

Fig. 1.

Behavioral Testing of Mice Submitted to a 28-Day Chronic Stress Protocol. (a) After two weeks of acclimatization, mice were placed on a polyphenol-free (PP-free) diet for an additional two weeks, followed by two weeks of pretreatment (control, BDPP, probiotic or synbiotic). Treatment therein continued throughout the duration of the protocol. At day 1, the CUS protocol began with twice daily mild unpredictable stressors. Behavioral testing was conducted following 26 days of stress (open field test for anxiety-like behavior, Fig. 1b) and 28 days (forced swim test for depressive-like behavior, Fig. 1c) after which mice were immediately sacrificed. Each group contained $n = 15$ mice mean +/− SEM with significance analyzed with two-way ANOVA calculations and Tukey posthoc analyses, $*p < 0.05$ and $**p < 0.01$.

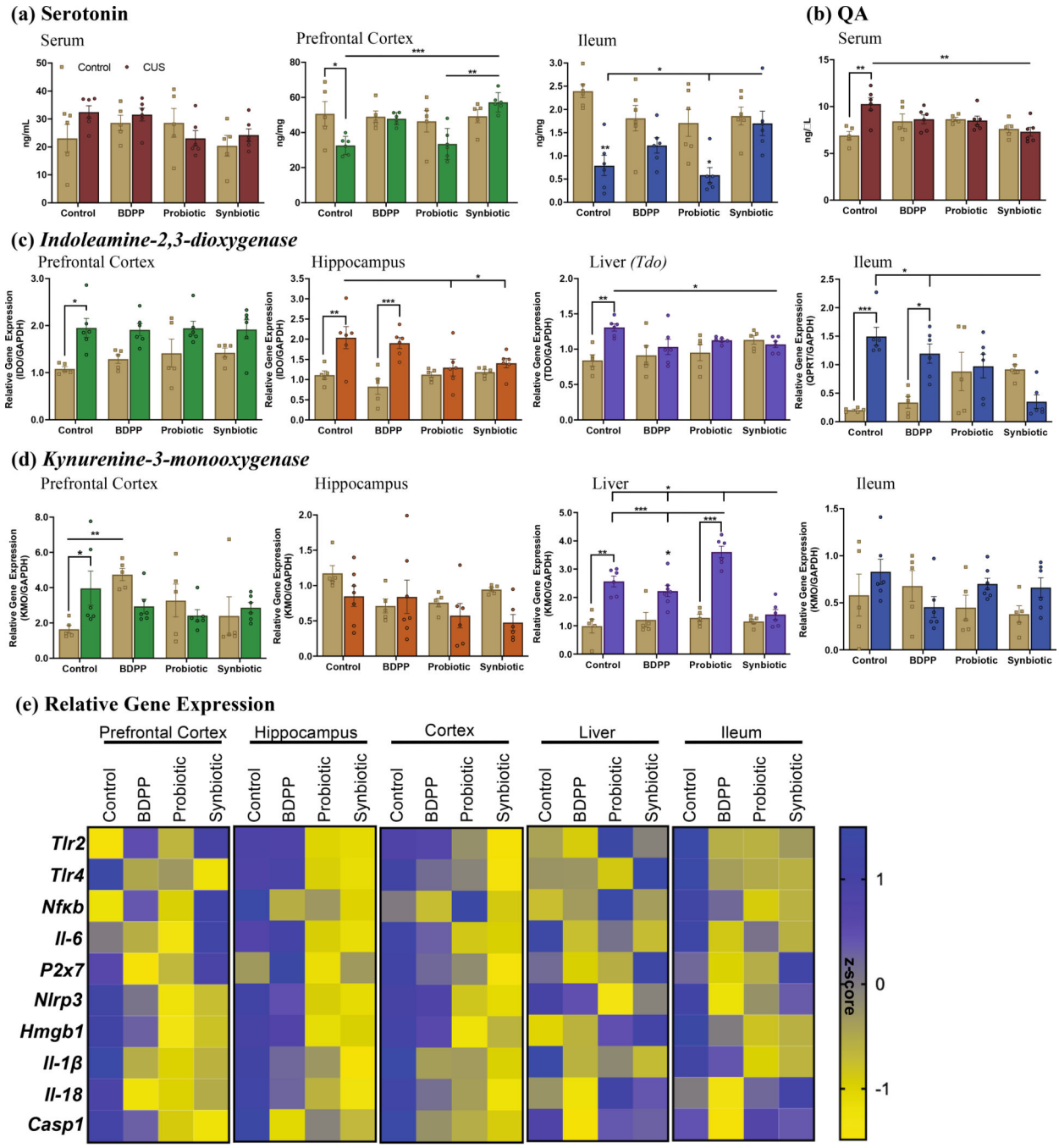

Fig. 2.

Disparate Regulation of Serotonin, Kynurenine Metabolism and Immune Signaling in Synbiotic-Treated CUS Mice. (a) Serotonin levels in the serum, prefrontal cortex and ileum and (b) quinolinic acid (QA) levels in the serum, were measured by ELISA assays in unstressed and stressed mice. ELISA analyses in the prefrontal cortex and ileum are reported normalized to the protein content in the sample while serum based ELISA to the volume of serum. mRNA expression of (c) indolamine-2,3-dioxygenase (*Ido*), and (d) kynurenine 3-monooxygenase (*Kmo*) in the prefrontal cortex, hippocampus, liver or ileum was measured

by real-time PCR and expressed as relative gene expression to the standard GAPDH using the $2^{-\Delta\Delta CT}$ method. Regulation of the immune system was indicated by cytokine expression (Fig. S2) and (e) gene expression of key immune regulatory factors. Heat map values are the ratio of stressed vs. non-stressed group within the respective treatment group, represented as row z-score of relative gene expression to GAPDH. Each value represents $n = 6$ independent samples mean +/− SEM with two-way ANOVA calculations and Tukey posthoc analyses where $*p < 0.05$, $**p < 0.01$ and ***p < 0.001.

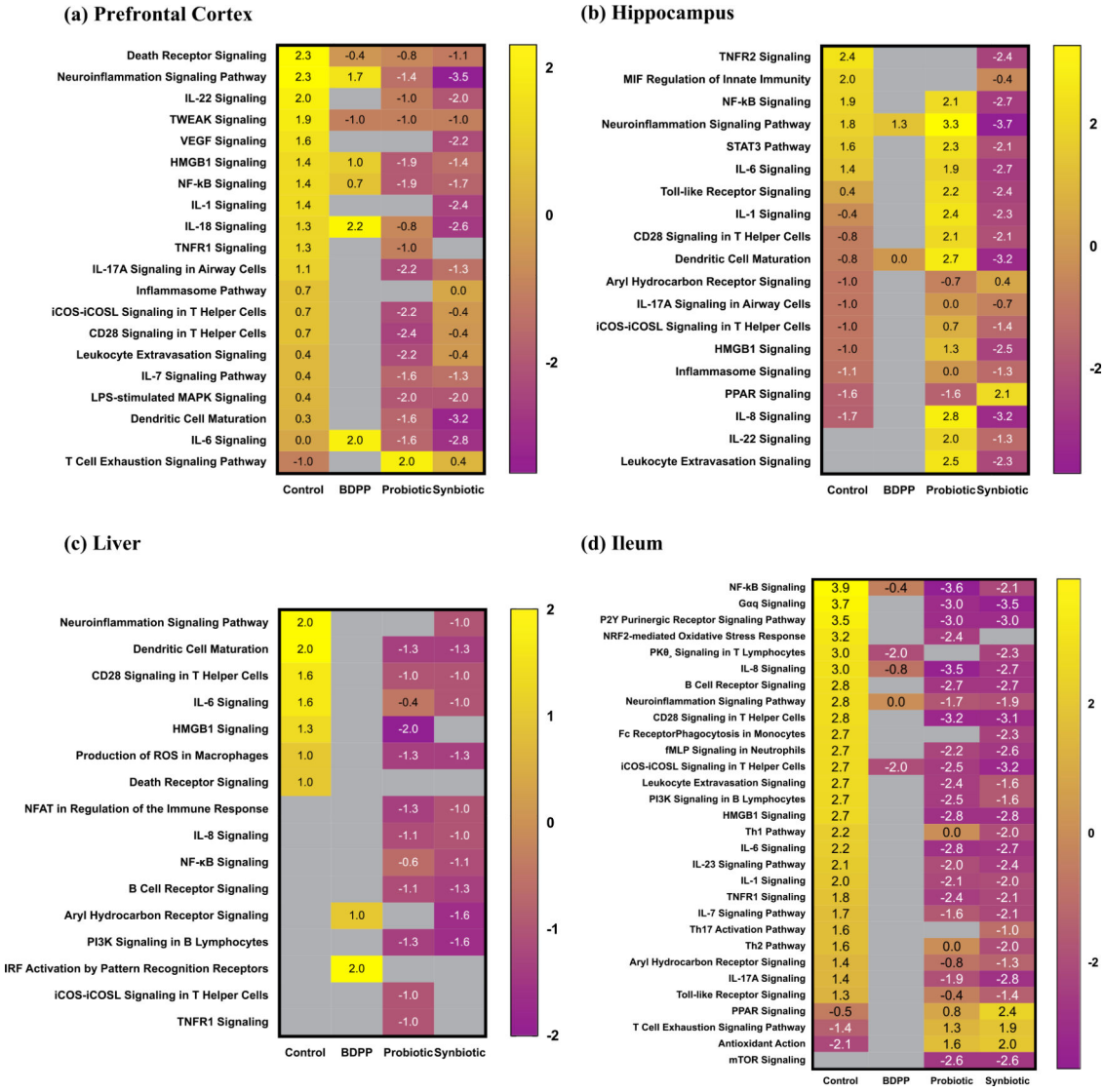

Fig. 3.

Integrated Pathway Analysis of Stress-Induced Canonical Pathways Affected by Treatment Groups Using NanoString Differential Expression. Gene expression analysis was conducted as the relative gene expression of each of the stressed groups compared to the unstressed control. Based on this data, major canonical pathways were determined by treatment groups in the (a) prefrontal cortex, (b) hippocampus, (c) liver and (d) ileum of CUS controls and synbiotic-treated CUS mice were determined using Qiagen's Integrated Pathway Analysis (IPA) Software. Expression is represented as the z-score of fold change between stressed vs. unstressed for the control samples, or treated stress vs. untreated stress for the BDPP, probiotic and synbiotic groups. Each group contains $n = 4$ independent samples with canonical pathway significance cutoff at $p < 0.05$.

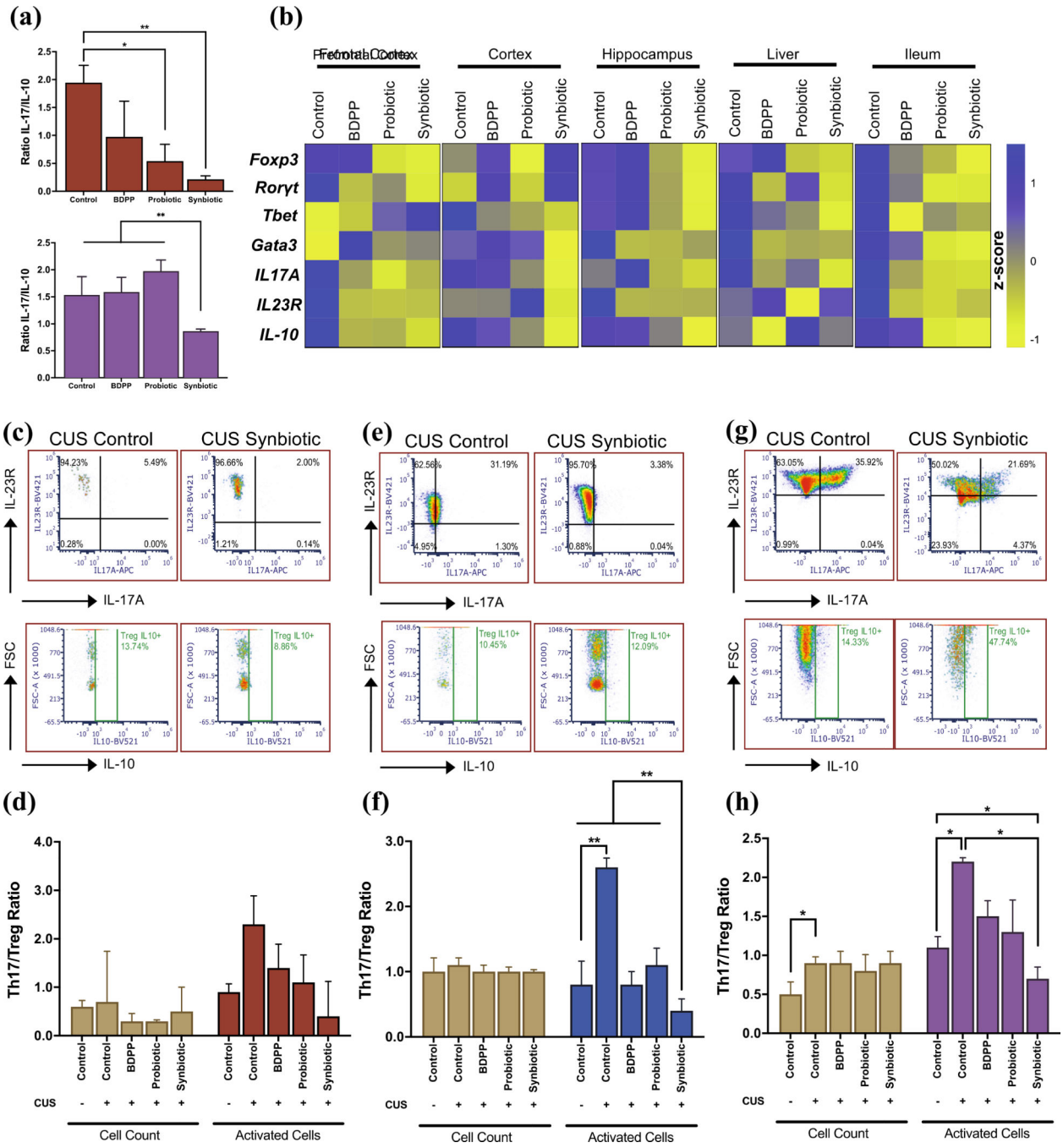

Fig. 4.

Stress-Induced Increase in the Th17 to Treg Ratio is Ameliorated by Synbiotic Treatment. The activity of the T helper (Th)17/Regulatory T (Treg) cells was determined by (a) ELISA assay of IL-17/IL-10 in the serum (upper) and ileum (lower) represented as the ratio of cytokine expression of stressed animals. (b) Gene expression analysis of key cell-type specific transcription factors in the prefrontal cortex, cortex, hippocampus, liver and ileum confirmed a shift in peripheral cell type populations. FACS analysis confirmed the treatment-dependent effects on stress-induced variations in activated Th17 ($CD3^+$

$CD4^+Ror\gamma t^+IL17A^+IL23R^+$) and Treg ($CD3^+CD4^+$ $Foxp3^+$ $IL10^+$) in the serum (c,d), liver (e,f) and ileum (g,h), compared to the unstressed vehicle control. ELISA and qpcr results represent $n = 6$ independent samples mean +/− SEM whereas FACS plots are representative of $n = 3$ independent samples mean +/− SEM. Significance was calculated with the student's *t*-test, $*p < 0.05$ and $**p < 0.01$.

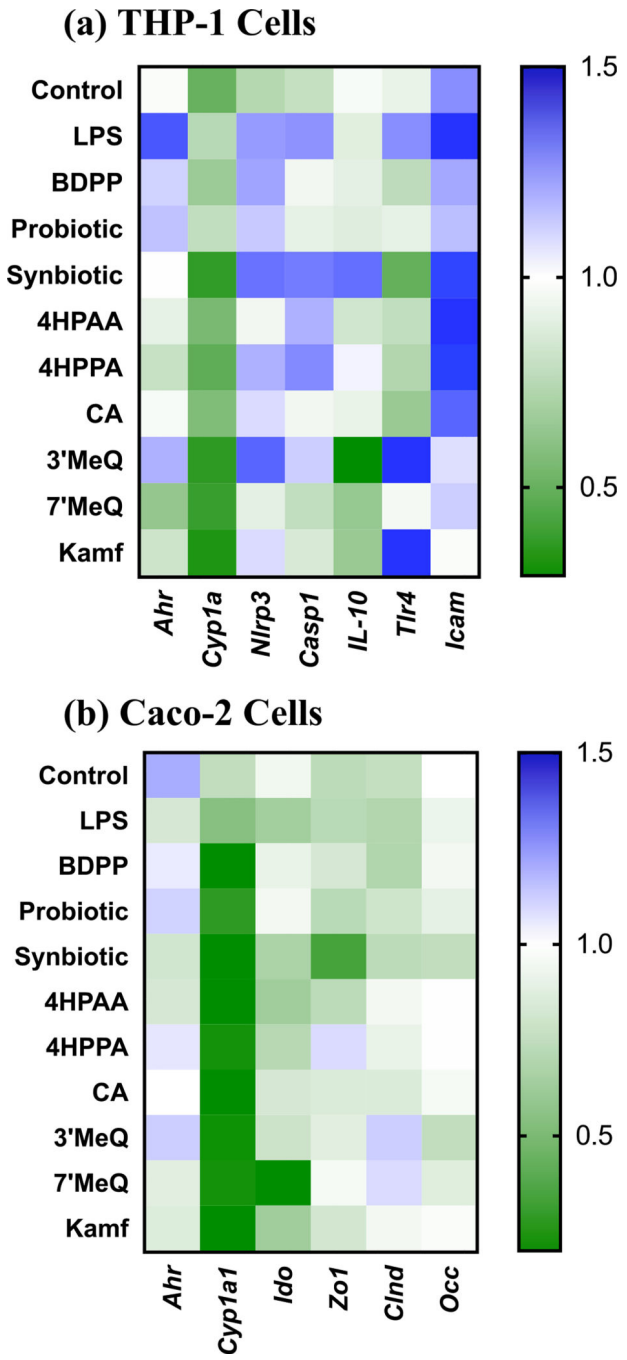

Fig. 5.

In vitro Coculture Verification of Aryl Hydrocarbon Receptor activity in Immune Cell Activation in Response to Treatment. With the same design as Table 2, gene expression of key immune or epithelial barrier genes in (a) THP-1 cells or (b) Caco-2 cells is shown as the z-score of fold change of TMF-treated vs. untreated groups. Each group represents the mean of $n = 4$ independent wells.

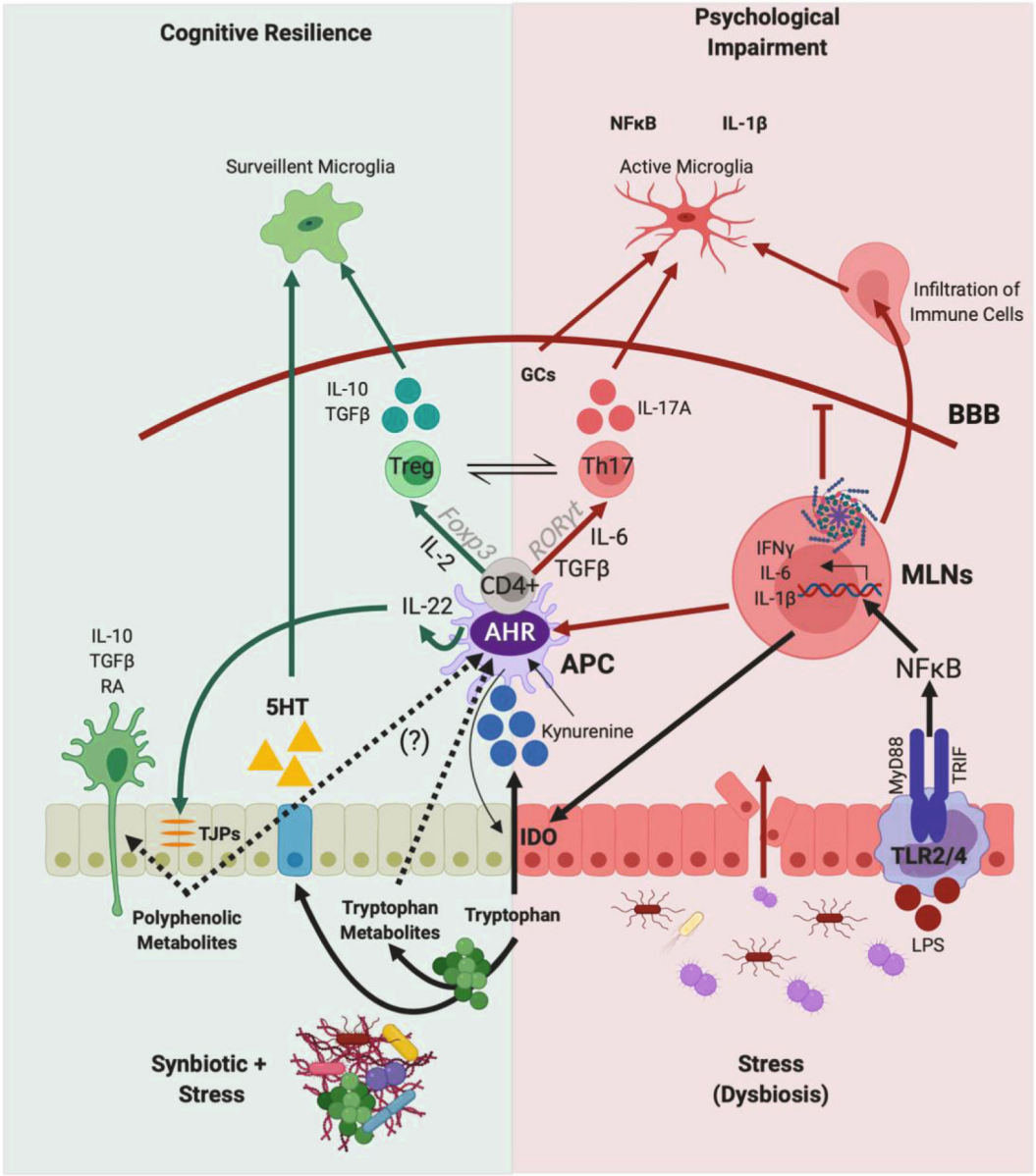

Fig. 6.

Scheme of Synbiotic-Derived Metabolites' Action on AHR-Mediated Treg/Th17 Ratios for the Promotion of Cognitive Resilience in Response to Stress. Synbiotic-derived metabolites promote cognitive resilience to stress-induced anxiety and depression by altering tryptophan metabolism, modulating aryl hydrocarbon receptor (AHR) activity and/or affecting the inflammatory activity of antigen presenting cells residing in the gastrointestinal associated lymphoid tissue (GALT). These effects inhibit the typical stress-induced induction of the innate immune response including NF-κB induction and proinflammatory cytokine production from peripheral immune cells in the mesenteric lymph nodes (MLNs) that ultimately interrupt blood–brain-barrier (BBB) integrity leading to the activation of microglia and cognitive impairment. Previously undefined acronyms: TJP – tight junction

protein, APC – antigen presenting cell, 5HT – serotonin, GCs – glucocorticoids, RA – retinoic acid.

Table 1

Pharmacokinetic Parameters of Polyphenols and Phenolic Acid Metabolites in Plasma and Brain Following 14-Day BDPP and Synbiotic Administration

Class	Metabolite	Chronic BDPP			Chronic Synbiotic		
		C_{max} (ng/ml)	T_{max} (h)	AUC (ng/mL*h)	C_{max} (pg/ml)	T_{max} (h)	AUC (ng/mL*h)
Plasma							
Phenolic Acids	PA	455089.0 ± 14664.0	0.5	8626346.0	602015.0 ± 213115.0	4.0	8803421.0
	3-HBA	20.2 ± 0.7	1.0	365.7*	12.5 ± 0.8	1.0	213.9
	4-HBA	71.2 ± 4.1	0.5	865.9	65.0 ± 8.3	24.0	1276.0**
	3-HPAA	113.0 ± 6.9	1.0	605.9	150.7 ± 35.6	0.3	1078.5**
	4-HPAA	297.3 ± 36.9	0.5	3755.3	220.6 ± 16.9	0.3	4456.6
	3,4-diHBA	76.4 ± 20.7	0.3	137.8**	28.8 ± 16.9	0.3	33.4
	4-HCA	118.4 ± 10.9	0.3	454.5	313.4 ± 40.8	0.3	1667.8**
	3-HPPA	4.0 ± 0.9	1.0	4.7	7.1 ± 1.0	2.0	60.0**
	4-HPPA	68.5 ± 13.7	0.5	405.7	480.6 ± 89.3	0.3	2169.8**
	3,4-diHPAA	67.2 ± 4.1	0.5	739.9**	19.4 ± 5.2	0.5	344.2
	VA	55.6 ± 2.4	0.5	299.2*	32.4 ± 32.4	0.3	118.4
	GA	1217.4 ± 199.8	0.3	1269.0	1253.4 ± 215.9	0.5	2387.3*
	HA	94.5 ± 18.3	1.0	889.3	99.3 ± 65.0	4.0	1316.6*
	CA	20.4 ± 3.6	0.3	52.8	69.9 ± 16.2	0.3	51.4
	HVA	21.1 ± 3.6	1.0	204.5	124.1 ± 23.8	0.5	1465.6**
	4-MeGA	154.8 ±14.3	0.5	336.0*	123.5 ± 24.5	0.5	162.5
	FA	28.9 ± 9.7	0.5	320.9**	22.6 ± 6.2	0.5	138.8
	4-HHA	2.1 ± 0.5	0.3	1.7	1.2 ± 0.3	2.0	5.9*
	DHFA	2.5 ± 0.7	0.3	30.7	7.7 ± 1.1	0.3	30.2
	DHVL	3.3 ± 0.4	0.5	123.4	21.2 ± 1.8	1.0	224.3*
Stilbene	RSV	11628.0 ± 1788.0	0.5	51313.0*	15785.0 ± 4246.0	0.5	33150.7
	DHRSV	122.8 ± 34.6	1.0	1049.3	593.0 ± 104.0	8.0	7796.6**
Flavonol	KAMF	5.6 ± 2.0	0.3	3.5	21.5 ± 3.7	0.5	38.2**
	QUER	41.7 ± 8.3	0.3	46.1	793.1 ± 715.9	0.3	583.4**
	3′-MeQUER	15.5 ± 1.4	0.25	15.6	20.5 ± 4.6	0.5	72.4**
	7′-MeQUER	n/a	n/a	n/a	0.03 ± 0.002	0.5	0.4

Class	Metabolite	Chronic BDPP			Chronic Synbiotic		
		C_{max} (ng/ml)	T_{max} (h)	AUC (ng/mL*h)	C_{max} (pg/ml)	T_{max} (h)	AUC (ng/mL*h)
Flavan-3-ol	MYR	57.7 ± 8.1	0.5	85.3	93.2 ± 22.8	0.3	305.1**
	C	55.5 ± 7.8	0.5	80.6**	9.8 ± 0.7	1.0	25.2
	EC	75.2 ± 12.7	0.3	188.7	123.7 ± 29.0	0.3	413.0**
	Me-C	31.4 ± 2.9	0.5	75.8**	17.4 ± 6.9	1.0	31.5
	Me-EC	33.0 ± 2.9	0.5	51.1	49.1 ± 8.5	0.5	88.5*
	PAC-B2	2.0 ± 0.7	0.5	1.5	2.7 ± 0.8	0.5	3.5*
Brain							
Phenolic Acids	PA	447100.0 ± 37200.0	0.5	6966231.0	759600.0 ± 140300.0	8.0	14499269.0**
	3-HBA	5.4 ± 0.4	0.5	67.3	8.9 ± 1.8	4.0	146.4**
	4-HBA	108.1 ± 19.3	0.0	1704.0	448 ± 15.0	8.0	6683.8**
	3-HPAA	2.7 ± 0.3	0.5	29.0	3.2 ± 0.5	0.5	41.2*
	4-HPAA	66.8 ± 4.7	1.0	1348.4	107.5 ± 6.5	1.0	1646.0*
	3,4-diHBA	15.2 ± 3.1	0.3	88.1	14.4 ± 3.8	0.5	291.2**
	3,4-diHPAA	100.0 ± 7.0	1.0	2204.1	126 ± 24.0	2.0	2115.1
	VA	9.7 ± 1.0	0.3	169.2	13.9 ± 1.8	1.0	205.0*
	GA	1344.0 ± 611.0	0.3	7559.8*	336.0 ± 112.0	2.0	4762.2
	HA	22.4 ± 11.6	1.0	518.1	111.4 ± 7.2	8.0	1814.7**
	HVA	296 ± 10.0	1.0	5922.9	301.0 ± 14.0	1.0	6222.3
	4-MeGA	2.2 ± 0.4	0.5	3.3	5.0 ± 1.0	0.3	6.8
	FA	1.5 ± 0.3	0.5	18.8	2.3 ± 0.6	2.0	20.0
Stilbene	RSV	9.5 ± 2.5	0.3	122.3**	3.8 ± 0.2	2.0	33.1
Flavonol	KAMF	25.3 ± 9.6	0.3	87.2	23.0 ± 2.6	1.0	288.4**
	QUER	89.5 ± 48.3	0.3	142.2	98.6 ± 24.7	2.0	544.3**
	3′-MeQUER	12.2 ± 6.9	0.3	26.9	28.4 ± 6.3	1.0	103.2**
	7′-MeQUER	n/a	n/a	n/a	0.1 ± 0.09	0.5	1.14
	MYR	86.5 ± 38.0	0.3	97.8	117.9 ± 18.0	1.0	578.2**

Table 2

In vitro Coculture Verification of Aryl Hydrocarbon Receptor activity in Immune Cell Activation in Response to Treatment

Metabolite	Treatment		TEER (% Control)	Cytotoxicity (% Change)	Kynurenine (% Change)	IL-1β(Fold Change)
	LPS	TMF				
Control	−	−	100.0 ± 2.4	99.4 ± 10.1	102.0 ± 1.6	1.00 ± 0.40
	−	+	101.2 ± 1.3	101.2 ± 2.2	105.9 ± 1.9	1.65 ± 0.23
LPS	+	−	67.0 ± 8.2	159.6 ± 10.3	120.5 ± 3.0	12.0 ± 3.2
	+	+	71.6 ± 5.2	134.3 ± 4.4*	125.0 ± 3.8	12.7 ± 0.5
BDPP	+	−	84.8 ± 3.8τ	129.1 ± 5.7τ	85.9 ± 2.7τ	8.1 ± 0.3τ
	+	+	75.4 ± 3.3*	130.4 ± 4.4τ	82.6 ± 4.7τ	7.3 ± 0.3τ
Probiotic	+	−	85.6 ± 2.0τ	90.4 ± 4.3τ	86.0 ± 1.8τ	7.5 ± 0.3τ
	+	+	77.4 ± 1.2	103.4 ± 1.1τ*	92.9 ± 1.6τ*	10.6 ± 0.7**
Synbiotic	+	−	93.2 ± 3.3τ	106.1 ± 1.5τ	89.0 ± 3.7τ	7.7 ± 0.2τ
	+	+	72.4 ± 2.2**	117.0 ± 2.5τ**	120.7 ± 7.9 **	11.0 ± 0.3**
4HPAA	+	−	87.3 ± 2.2τ	112.9 ± 0.9τ	89.0 ± 3.7τ	5.2 ± 0.6τ
	+	+	70.2 ± 2.0**	139.5 ± 4.6*	120.7 ± 7.9**	9.8 ± 0.4τ**
4HPPA	+	−	85.6 ± 1.2τ	106.8 ± 6.7τ	102.0 ± 2.2τ	6.4 ± 0.3τ
	+	+	72.3 ± 2.0**	133.3 ± 5.0τ*	134.3 ± 3.2**	9.1 ± 0.0τ**
CA	+	−	80.2 ± 3.2τ	98.6 ± 5.0τ	98.6 ± 7.7τ	4.0 ± 0.3τ
	+	+	73.2 ± 0.9*	162.7 ± 3.4**	144.1 ± 6.4**	10.3 ± 0.3τ**
3′MeQ	+	−	77.0 ± 0.9τ	133.4 ± 10.4τ	102.3 ± 9.6τ	6.5 ± 0.4τ
	+	+	73.4 ± 1.2	170.3 ± 18.4	129.9 ± 13.8	9.4 ± 0.3τ*
7′MeQ	+	−	79.2 ± 1.1τ	123.4 ± 3.3τ	119.5 ± 4.3	7.9 ± 0.4τ
	+	+	74.5 ± 2.0	145.3 ± 9.4	132.0 ± 13.3	8.1 ± 0.4τ
Kamf	+	−	83.0 ± 2.0τ	121.5 ± 5.6τ	151.0 ± 3.7	8.4 ± 0.2τ
	+	+	75.5 ± 2.1*	108.2 ± 9.7τ	131.7 ± 3.9	10.1 ± 0.7τ

Cocultures of human colorectal adenocarcinoma (Caco-2) and phorbyl 12-myristate 13-acetate (PMA)-activated human monocyte (THP1) cells were pretreated with the supernatant of 24 h fermented BDPP, probiotic or synbiotic solutions or specific metabolites (250 ng/mL) for 24 h before stimulation with LPS, IFNγ and ATP for 8 h. Wells were also treated with or without 6, 2, 4’-trimethoxyflavone (TMF), a potent AHR antagonist. Treatment- and TMF-induced variations in transepithelial electrical resistance (TEER), cytotoxity measured with an lactate dehydrogenase (LDH) release assay, kynurenine with a chemical assay and IL-1b with ELISA. TEER, cytotoxicity and kynurenine are represented as percentage of control while IL-1b is fold change from untreated controls. Each sample has $n = 4$ independent samples mean +/− SEM, significance calculated with a student’s t-test

* $p<0.05$

** $p<0.01$ within the same treatment group and t $p<0.05$ compared to LPS-treated control (highlighted in grey).